DURBAN UNIVERSITY OF TECHNOLOGY

THE SYNTHESIS, STRUCTURE AND PROPERTIES OF POLYPROPYLENE NANOCOMPOSITES

VISHNU KRIBAGARAN MOODLEY

THE SYNTHESIS, STRUCTURE AND PROPERTIES OF POLYPROPYLENE NANOCOMPOSITES

A THESIS SUBMITTED TO THE

DURBAN UNIVERSITY OF TECHNOLOGY

FOR THE MASTER OF TECHNOLOGY DEGREE

(IN MECHANICAL ENGINEERING)

BY

VISHNU KRIBAGARAN MOODLEY

DEPARTMENT OF MECHANICAL ENGINEERING

FACULTY OF ENGINEERING, SCIENCE

AND THE BUILT ENVIRONMENT

DURBAN 4000, SOUTH AFRICA

SUPERVISOR: PROF K KANNY

2007

DECLARATION

This thesis is being submitted to the Durban University of Technology for the degree of Master of Technology (Mechanical Engineering). I declare that this work is my own and has not been submitted before for any degree or examination to any other university or institution.

_____

VISHNU KRIBAGARAN MOODLEY

Student No: 20358024

June 2007

FINAL APPROVED SUBMISSION

_____ _____

Prof K Kanny Date

ACKNOWLEDGEMENTS

This thesis grew out of a series of dialogues with my supervisor Professor Krishnan Kanny. Through his Socratic questioning, Prof. Kanny brought me closer to the reality I had initially perceived, eventually enabling me to grasp its rich complexity. I am also indebted in gratitude to Dr. Jawahar Paulraj, Avinash Ramsaroop and Santhesh Hiraman whose work in composites has inspired me. Prof. Kanny and Dr. Jawahar Paulraj's comments on chapter drafts are themselves a course in critical thought upon which I will always draw upon. Their capacity to combine critique with an immediate empathy and commitment towards my work will always inspire me. Prof. Kanny was at the centre of our friendships at the Mechanical Engineering Department inspiring me with his quick wit and incredible imagination. Amid the laughter and chapter drafts, Prof. Kanny was always there to offer quiet an encouragement, at times unturned by their his extraordinary kindness. I am very grateful for my years at the Durban University of Technology (DUT), made possible by the financial support of KENTRON through the HYSTOU 4 programme, the fund granted to me Research Management & Development Department on DUT and the steadfast support of my family. Many thanks to Mr Vijay Bandu (Chief Technician) for the transmission electron microscopy studies (TEM) and Mrs Belinda White (Chief Electron Microscope Technician) for the scanning electron microscope studies (SEM) who are both situated at the Centre for Electron Microscopy at University of Kwazulu Natal. Their editing suggestions and precise sense of language contributed to the morphological analysis of the study on nanocomposites. I give thanks to the staff at the DUT Mechanical Engineering Department, for their friendship and support to myself and other students from around the world. I am forever grateful to my grandmother,

whose foresight and values paved the way for a privileged education, and to my parents and brother who gently offer counsel and unconditional support at each turn of the road.

TABLE OF CONTENTS

ABSTRACT

Polymer nanocomposites may be defined as structures that are formed by infusing layered-silicate clay into a thermosetting or thermoplastic polymer matrix. The nanocomposites are normally particle-filled polymers for which at least one dimension of the dispersed particles is in nanoscale. These clay-polymer nanocomposites have thus attracted great interest in industry and academia due to their exhibition of remarkable enhancements in material properties when compared to the virgin polymer or conventional micro and macro-composites.

The present work describes the synthesis, mechanical properties and morphology of nano-phased polypropylene structures. The structures were manufactured by melt-blending low weight percentages of montmorillonite (MMT) nanoclays (0.5, 1, 2, 3, 5 wt. %) and polypropylene (PP) thermoplastic. Both virgin and infused polypropylene structures were then subjected to quasi-static tensile tests, flexural tests, micro-hardness tests, impact testing, compression testing, fracture toughness analysis, dynamic mechanical analysis, tribological testing. Scanning electron microscopy studies were then conducted to analyse the fracture surfaces of pristine PP and PP nanocomposite. X-ray diffraction studies were performed on closite 15A clay and polypropylene composites containing 0.5, 1, 2, 3 and 5 wt. % closite 15A nanoclay to confirm the formation of nanocomposites on the addition of organo clays. Transmission electron miscopy studies were then performed on the PP nanocomposites to determine the formation of intercalated, exfoliated or agglomerated nanoclay structures.

Analysis of test data show that the mechanical properties increase with an increase in nanoclay loading up to a threshold of 2 wt. %, thereafter the material properties degrade. At low weight nanoclay loadings the enhancement of properties is attributed to the lower percolation points created by the high aspect ratio nanoclays. The increase in properties may also be attributed to the formation of intercalated and exfoliated nanocomposite structures formed at these loadings of clay. At higher weight loading, degradation in mechanical properties may be attributed to the formation of agglomerated clay tactoids. Results of XRD, transmission electron microscopy studies and scanning electron microscopy studies of the fractured surface of tensile specimens verify these hypotheses.

LIST OF FIGURES

FIGURE **PAGE**

continued,

FIGURE **PAGE**

continued,

FIGURE **PAGE**

LIST OF TABLES

TABLE **PAGE**

CHAPTER 1

INTRODUCTION

1.1. COMPOSITES

Man has used a variety of materials for their needs and comfort. They have also developed new materials for meeting their technological requirements. As the levels of technology become more and more sophisticated, the materials used are to be correspondingly more efficient. Several performance characteristics are expected from these materials. Firstly, the materials for high-end applications, such as aerospace engineering, should have higher performance efficiency and reliability. Secondly, materials have to be light weight for many applications such as thermoplastic storage compartments used in airplanes, so that the resulting products can be energy efficient and cost effective. At least 40 per cent of the cost of any engineered product is constituted by the cost of materials used for its construction, as in the automotive and polymer industries. Thirdly, materials must have a good combination of properties, such as tensile and flexural strength. This suggests that an engineer must be able to design the material system with combinations of properties for specific end uses. Finally, the present day products of modern technological origin may operate in environments that are special or extreme, like very high temperature (of the order of 2500K), cryogenic conditions, highly corrosive, vacuum (as in space), high hydrostatic pressure (as in deep sea), high electric, magnetic or irradiation fields, etc. The conventional materials may not always be capable of meeting the demands of such environments. New materials are being created for meeting these performance requirements and composite materials form one class of such material system developed.

Composite material has a complex morphology, in which two or more distinct, structurally complementary substances combine to produce some structural or functional properties not present in any individual component. Examples of this are, glass fiber reinforced thermoset polymers, and wood (a water-plasticized, air-foamed composite of cellulose fibres in a crosslinked lignin matrix). In engineering and material science, composites are more narrowly defined as physical mixtures of chemically different materials that are insoluble in each other and are thus present as distinct phases: usually a continuous phase (matrix), and a discontinuous phase.

1.2. CLASSIFICATION OF COMPOSITES

Composites may be classified into different types based on the reinforcement and the matrix that are used.

1.2.1. Classification Based on Reinforcements

Composites can be classified as particle-reinforced composites and fiber-reinforced composites based on the type of reinforcing particles [1]. Composites, in which the dispersed reinforcing phase is present in the form of particles is called particle-reinforced composites. The particle-reinforced composites can be further classified into large-particle composites and dispersion-strengthened composites based on particle size. The distinction between these is based upon reinforcement size, and strengthening mechanism. The term “large” is used to indicate that, the particle-matrix interaction cannot be treated in molecular or atomic level. For most of these composites the particulate phase is stronger than the matrix. These reinforcing particles tend to restrain the movement of the matrix phase in the vicinity of each particle. In essence, the matrix transfers some of the applied stress to the particles, which bears a fraction of the load. The degree of reinforcement or improvement of the

mechanical behavior depends upon the strong bonding at the matrix-particle interface. The particles are small in size (10 –100 nm) in the dispersion-strengthened composites. Particle-matrix interactions that lead to strengthening occurs at the atomic level. The matrix bears the major portion of an applied load, and the small-dispersed particles, hinder or impedes the motion of dislocations. Thus, plastic deformation is restricted such that yield strength, tensile strength and hardness improve.

Composites where the dispersed reinforcing phase is in the form of fiber are called fiber-reinforced composites (FRC). Based on fiber alignment and length, the FRC can be classified further into three categories [2],

1. Continuous and aligned FRC
2. Discontinuous and aligned FRC
3. Discontinuous and randomly oriented FRC

In continuous and aligned FRC the fibers are continuous and aligned. The properties of a composite having its fibers aligned are anisotropic, (i.e.) dependent on the direction in which they are measured. In discontinuous and aligned FRC the fibers are discontinuous and aligned in one direction. The reinforcement efficiency will be lower for discontinuous and aligned FRC compared to continuous and aligned FRC. It will approach 90 per cent of elastic moduli, and 50 per cent of tensile strength of continuous and aligned FRC [2]. Discontinuous and randomly oriented FRC can be considered as an isotropic material. It exhibits uniform property in all directions. The fibers are short, discontinuous, and randomly oriented.

1.2.2. Classification Based on Matrix

Based on matrix material [3] the composites can be classified as:

1. Polymer Matrix Composites (PMC)

2. Metal Matrix Composites (MMC)
3. Ceramic Matrix Composites (CMC)

In polymer matrix composites, the matrix phase is polymer and the reinforcing phase may be fibers or ceramic particles. These materials are used in various composite applications e.g. aerospace engineering and are used in sizeable quantities because of their low cost and ease of fabrication.

For the polymers in solid state, the polymer chains become entangled and the portion of the polymer molecules can pack closely together. In some polymers this packing becomes close and even secondary bonds form between polymers. These areas of close packing are called crystalline regions because of its analogy with metallic and ceramic crystals. In some polymers the molecules do not closely pack and they are randomly arranged. These regions are called amorphous regions. Most of the thermoplastic polymers are semi-crystalline and thermoset polymers are amorphous. These thermoplastic polymers exhibit medium strength, easy to process, recyclable, flow under the application of temperature, and have poor heat resistance. Thermosetting polymers exhibit better strength compared to the thermoplastic polymers, are easy to process, rigid, have better heat resistance, hardens on application of temperature, and are non- recyclable. Even though the polymers exhibit better properties, they have certain drawbacks compared to other material systems like metals and ceramics. These polymer materials are only meant for low strength and low temperature applications. In order to extend its usage in structural areas, these polymeric materials are filled with fillers and reinforcements, so that it can withstand high strength and also have high glass transition temperature. Because of this, the polymer composites are preferred to polymers in many engineering applications.

As the name implies, for metal matrix composites, the matrix is a ductile metal or alloy and the reinforcing medium is continuous like fibers of carbon, silicon carbide, boron and alumina. Discontinuous reinforcement includes silicon carbide whiskers, chopped fibers of carbon and alumina, particulates of silicon carbide and alumina. These materials may be utilized at higher service temperature than their base counterparts. These materials are nonflammable and have greater resistance to organic fluids. Therefore, metal matrix composites are more expensive than polymer matrix composites.

In ceramic matrix composites, particulates, fibers or whiskers of one ceramic material are embedded into the matrix of another ceramic material. These ceramic composites have improved fracture toughness and high stress application compared to the ceramic material alone. Ceramic composite materials are meant for high temperature applications like heat shield of re-entry spacecrafts.

The present research work mainly deals with polymer composite materials with more emphasis given to nanocomposites structures.

1.3. CLASSIFICATION OF POLYMER COMPOSITES

Polymer composites can be classified as

1. Macro-composites
2. Micro-composites
3. Nanocomposites

Polymer macro-composites are heterogeneous composites of polymers and “macro” sized fillers. The reinforcing phase in macro-composites will be in the millimeter range. Polymer concrete is composed of polymers (polyester or poly methyl

methacrylate), aggregates (sand, ground limestone, etc.), and other additives (dyes, etc.). But it does not contain cement. Compositional boards are panel products. They include particleboard, fiberboard, and hard board from flakes or shearing chips, etc. The fillers are mainly wood products and the resin used is urea formaldehyde, polyurethane or phenolic resin.

Composites employing micron size fibers with high aspect ratio or fine hollow spheres or fibers as reinforcement are called micro composites. Here the matrix may be any polymer. The reinforcing phase will be a continuous fiber or short fiber or micron sized fillers such as silicon carbide, alumina, etc. The main advantage of using fibers is to improve strength, stiffness, and thermal stability of composites.

In nanocomposites, the reinforcing phase will be in the nanometer range. Generally macroscopic reinforcing elements contain imperfections. Structural perfection increases as the reinforcing elements become smaller and smaller. The ultimate properties of reinforcing composite elements may be expected when their dimension reach atomic or molecular levels. For example, carbon nanotubes have the highest elastic modulus (1 TPa). In comparison, individual clay sheets, being only 1 nm thick and constructed from only three metal oxide layers, display a perfect crystalline structure and have better properties.

In nanocomposites, the reinforcing nanomaterial may be,

1. Three-dimensional nanomaterials: all dimensions of the material are in the order of nanometers (e.g. spherical alumina nanoparticles)
2. Two-dimensional nanomaterials: two dimensions of the material are in nanometer range (e.g. carbon nanotube or whiskers)
3. One-dimensional nanomaterials: only one dimension of the material is in nanometer range. (e.g. clay).

At these very small sizes, the property of nanocomposites depends not only on the properties of two materials that form them but also on the way these materials interact together at the molecular level. Clearly, the interfaces between the matrix and reinforcement are maximized in nanocomposites. Hence, the properties of the composites, that is especially dependent on interfacial strengths, such as shear strength, and very high flexural strength. The mechanical and electrical properties can be simultaneously maximized in such composite materials to achieve super conducting structural material. Other properties that have been shown to be superior in nanocomposites were optical clarity, thermal stability, and reduced flammability [4].

1.4. CLAY POLYMER COMPOSITES

Recently clays are considered as a fundamental reinforcing element in nanocomposites [5]. Clay-polymer nanocomposites are a relatively new class of reinforced polymers with incorporated particles that are about 1000 times smaller than those in conventional composites. In clay-polymer nanocomposites, the silicate platelets are dispersed much more finely. Dimensions of silicate platelets are of the order of 1 nm thick, and width, and length in the range of 100-200 nm. Surface areas of the clays are approximately 700 m^2 per gram. The silicate platelets in clay-polymer nanocomposites are not only small, but also the aspect ratio (length/thickness) is much higher.

These clay-polymer nanocomposites possess a unique combination of properties, i.e. relatively high strength, and stiffness, high barrier properties, and good flame retardancy. The processibility is similar to that of unfilled polymers and conventional

polymer composites. It also offers extra benefits like low density, transparency, good flow, better surface properties, improved dimensional stability, and recyclability [5].

1.5. APPLICATIONS OF NANOCOMPOSITES

The clay-polymer nanocomposites may be used in various automotive, general and industrial applications. These include potential for utilization as mirror housings on various vehicle types, door handles, engine covers, and intake manifolds, and timing belt covers. More general applications currently being considered include usage as impellers, and blades for vacuum cleaners, power tool housings, and covers for portable electronic equipment such as mobile phones, pagers etc [6].

Clay nanoparticles, for instance, are of new relevance to materials, due to their ability to make the materials stronger, lighter, more durable, and transparent. These materials are already being applied in the US automotive industry; the GM Motors, Safari and Chevrolet Astro vans, for instance, use a clay-polypropylene nanocomposite material for a ‘step-assist’, an optional extra to improve access to the vehicle. Mitsubishi’s GDI cover for engines is made of clay/nylon-6 nanocomposites [7].

Nanocomposites also find applications in both flexible and rigid food packaging. Specific examples include packaging for processed meats, cheese, confectionery, cereals, and boil-in-the-bag foods, also extrusion-coating applications in association with paperboard for fruit juice, and dairy products, together with co-extrusion processes in the manufacture of beer, and carbonated drinks bottles [6].

Nylon is often regarded as one of the most promising resins for nanocomposite additives [8]. In packaging, the major application focus for nylon 6 nanocomposites is in high-barrier packaging. The clay-polyethylene terepthalate nanocomposites bottles are also used as containers to hold drinks, since it has improved oxygen, and carbon

dioxide barrier [9]. Considerable interest is now being shown in clay-polyamide-6/66 nanocomposites as both fuel tank and fuel line components for cars [8].

1.6. PRESENT WORK

In the present work, clay-polymer nanocomposites are prepared using thermoplastic polypropylene as the matrix and organo-modified clay, Closite 15A, as the reinforcing phase. The clay-polypropylene nanocomposites morphology is characterized by X-ray diffraction studies (XRD) and transmission electron microscopy (TEM). The study of the mechanical properties of pristine and infused PP nanocomposites includes tensile, flexural, impact, hardness, and compression testing. The fracture surface analysis of polypropylene nanocomposites includes scanning electron microscopy and fracture toughness testing. The polypropylene nanocomposites were further analysed to determine the storage modulus by dynamic mechanical analysis (DMA) and the wear loss was determined by tribological analysis.

CHAPTER 2

LITERATURE REVIEW

2.1. CLAY POLYMER NANOCOMPOSITES

In recent years clay-polymer (CP) nanocomposites have attracted great interest, both in industry and in academia, because, they exhibit remarkable improvement in materials properties when compared to virgin polymer or conventional micro and macro-composites. These improvements include high moduli [10-14], increased strength, and heat resistance [15], decreased gas permeability [16-20] and flammability [21-25]. Biodegradability of biodegradable polymers is also enhanced due to the presence of terminal hydroxylated edge group in the silicate layers [26]. On the other hand, there has been considerable interest in theory and simulations addressing the preparation and properties of these materials [27-31], and they are also considered to be unique model systems to study the structure and dynamics of polymers in confined environments [32-34]. Although the intercalation chemistry of polymers when mixed with appropriately modified clay and synthetic clay has long been known [35], the field of clay polymer nanocomposites has gained momentum recently after the two major findings that have stimulated the revival of interest in these materials. First, the report from the Toyota research group of a Nylon-6 (N6)/montmorillonite (MMT) nanocomposite [36], for which very small amounts of clay loading resulted in pronounced improvements of thermal and mechanical properties. Second, the observation by Vaia et al., that it is possible to melt-mix polymers with clay without the use of organic solvents [37]. Today, efforts are being made globally to prepare nanocomposites using almost all types of polymer matrices.

2.2. STRUCTURE OF CLAY

The commonly used clay for the preparation of CP nanocomposites belongs to the general family of 2:1 layered silicates [38]. Its crystal structure consists of layers made up of two tetrahedrally coordinated silicon atoms fused to an edge-shared octahedral sheet of either aluminum or magnesium hydroxide. The layer thickness is around 1 nm, and the lateral dimensions of these layers may vary from 30 nm to several microns, depending on the particular clay. Stacking of the silicate layers leads to a regular van der Waals gap between the layers called the interlayer or gallery. Isomorphic substitution within the layers (for example, Al^{3+} replaced by Mg^{2+} or Fe^{2+}, or Mg^{2+} replaced by Li^{1+}) generates negative charges that are counterbalanced by alkali, and alkaline earth cations situated inside the galleries. This type of clay is characterized by a moderate surface charge known as the cation exchange capacity (CEC), and generally expressed as meq/100 g. This charge is locally constant, but varies from layer to layer, and must be considered as an average value over the whole crystal. Montmorillonite (MMT), hectorite, and saponite are the most commonly used clays.

Clays have two types of structure: tetrahedrally substituted and octahedrally substituted. In the case of tetrahedrally substituted clays the negative charge is located on the surface of silicate layers, and hence, the polymer matrices can interact more readily with these than with octahedrally substituted clay. Details regarding the structure and chemistry of these clays are provided in Fig. 2.1 and Table 2.1 respectively.

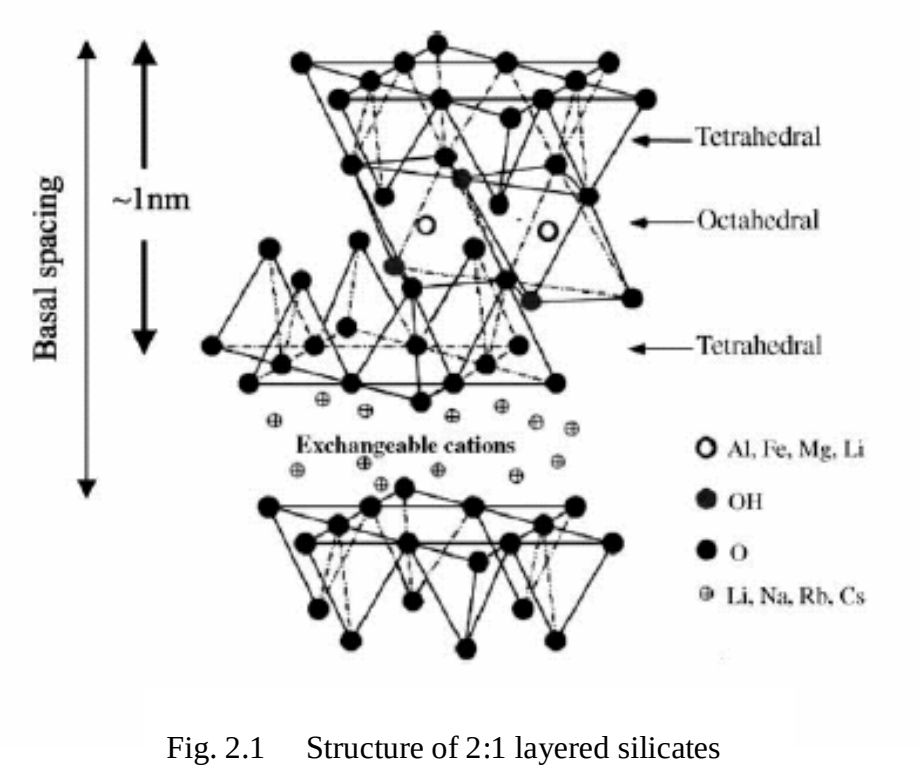

Fig. 2.1 Structure of 2:1 layered silicates

Table 2.1 Chemical formula and cation exchange capacity of commonly used 2:1 layered silicates

2:1 layered silicates	**Chemical formula**	**CEC (meq/100 g)**
Montmorillonite	$M_x(Al_{4-x}Mg_x)Si_8O_{20}(OH)_4$	110
Hectorite	$M_x(Mg_{6-x}Li_x)Si_8O_{20}(OH)_4$	120
Saponite	$M_xMg_6(Si_{8-x}Al_x)Si_8O20(OH)_4$	86.6

M is the monovalent cation and **x** the degree of isomorphous substitution (between 0.5 and 2.3).

Two particular characteristics of clays are generally considered for CP nanocomposites; the first is the ability of the silicate platelets to disperse into individual layers. The second characteristic is the ability to fine-tune their surface chemistry through ion exchange reactions with organic and inorganic cations. These two characteristics are, of course, interrelated since the degree of dispersion of silicate platelets in a particular polymer matrix depends on the interlayer cations.

2.3. CLAY SURFACE TREATMENTS

Pristine inorganic clay usually contains hydrated Na^+ or K^+ ions [39]. Obviously, in this pristine state, inorganic clays are only miscible with hydrophilic polymers, such as poly ethylene oxide (PEO) [40], or poly vinyl alcohol (PVA) [41]. To render silicate layers miscible with other polymer matrices, one must convert the normally hydrophilic silicate surface to an organophilic surface. There are different ways to modify clay minerals. The methods include adsorption, ion exchange with inorganic cations, ion exchange with organic cations, grafting of organic compounds, reaction with acids, pillaring by different types of poly hydroxo metal cations, polymerization, and physical treatments such as lyophilization, ultrasound, and plasma [42]. Ion exchange with alkyl ammonium ions is a well-known method to make clay minerals and clays dispersible in organic solvents and to render them compatible with hydrophobic materials during composite processing. Exchanging the interlayer cations of natural, and synthetic clay minerals (hectorites, fluoro micas, taeniolite), and alkali silicates will provide a simple method to prepare new types of organic–inorganic hybrid materials. Intercalation of organic compounds is usually performed by reacting the clay minerals with solutions or melts of the guest compounds. Among these, cation exchange by organo-onium ions is the simplest method to modify montmorillonite clays because of its high cation exchange capacity.

2.3.1. Cation-Exchange Process

A characteristic feature of montmorillonite is their ability to sorb certain cations and to retain them in an exchangeable state. It means that these intercalated cations can be exchanged by treatment of other cations in a water solution. The most common exchangeable cations are Na^+, Ca^{2+}, Mg^{2+}, H^+, K^+ and NH_4^+. If the clay is placed in a

solution of a given electrolyte, an exchange occurs between the ions of the clay (X^+) and those of the electrolyte (Y^+).

$$X.clay + Y^+ \rightleftharpoons Y.clay + X^+ \qquad (2.1)$$

As indicated, this reaction is balanced, and the extent to which the reaction proceeds from the left to the right depends on the nature of the cations X^+, and Y^+, on their relative concentrations, and often on secondary reactions.

Although the Law of Mass is not obeyed quantitatively in the equation (2.1), the equilibrium of the reaction can be moved to the right by increasing the concentration of the added Y^+ cation. The cation-exchange process is controlled by the diffusion of the ion replacing the existing resident ion on the cation-exchange site. It is considered to occur in two stages:

1. Diffusion from the bulk of the solution through the individual layers surrounding the clay particles
2. Diffusion within the particle itself (particle diffusion)

2.3.2. Cation-Exchange Capacity

For a given clay, the maximum amount of cations that can be taken up is constant and is known as the cation-exchange capacity (CEC). It is measured in milliequivalents per gram (meq/g) or more frequently per 100 g (meq/100g). Although the convention is to use this unit, in SI units it is expressed in “coulombs per unit mass”. A CEC of 1 meq/g is 96.5 C/g in SI units. Cation-exchange capacity measurements are performed at a neutral pH of 7. The CEC of montmorillonite varies from 80 to 150 meq/100g. Determination of the cation-exchange capacity is more or less arbitrary and no high

degree of accuracy can be claimed. The measurement is made by saturating the clay with NH_4^+ ions and determining the amount by conductometric titration.

2.3.3. Compatibilizing Agents

Dispersing clay in a polymer is like trying to mix oil in water. Clay is hydrophilic in nature, whereas most polymers are hydrophobic. The role of a compatibilizing agent is similar to that of detergents. It is a molecule constituted of one hydrophilic function (which likes polar media such as water or clay) and one organophilic function (which likes organic molecules such as oil or polymer). This allows the dispersion of clay in polymers.

The first compatibilizing agents used in the preparation of nanocomposites (Nylon 6-clay hybrids) were amino acids [43]. Numerous other kinds of compatibilizing agents have since been used in the synthesis of nanocomposites. The most popular are alkyl ammonium ions because they can be easily exchanged with the ions situated between the layers. Silanes have been used because of their ability to react with the hydroxyl groups situated possibly at the surface and at the edges of the clay layers. Other compatibilizing agents can also be used.

(a) Amino acids

Amino acids are molecules which consist of a basic amino group ($-NH_2$) and an acidic carboxyl group (-COOH). In an acidic medium, a proton is transferred from the $-COOH$ group to the intermolecular $-NH_2$ group. A cation-exchange is then possible between the $-NH_3^+$ functional group formed and a cation (i.e. Na^+, K^+) intercalated between the clay layers so that the clay becomes organophilic. A wide range of ω-amino acids ($COOH - (CH_2)_{n-1} - NH_3^+$) have been intercalated between the layers of montmorillonite. Amino acids were widely used in the preparation of clay-

nylon 6 hybrids because, the acid functional group has the ability to polymerize with ε- caprolactam intercalated between the layers [43]. This intergallery polymerization delaminates the clay in the polymer matrix and favors the nanocomposite formation.

(b) Alkylammonium ions

Montmorillonite exchanged with long chain alkylammonium ions can be dispersed in polar organic liquids, forming gel structures with high liquid content. Alkylammonium ions can be intercalated easily between the clay layers and offer a good alternative to amino acids for the preparation of nanocomposites based on polymer systems. The most widely used alkylammonium ions are based on primary alkyl amines put in an acidic medium to protonate the amine function. Their basic formula is CH_3-$(CH_2)_n$-NH_3^+ where n is between 1 and 18. It is interesting to note that the length of the ammonium ions has a strong impact on the resulting structure of nanocomposites. Lan et al. [44] showed that, alkylammonium ions with chain length larger than eight carbon atoms were favoring the formation of delaminated nanocomposites whereas alkylammonium ions with shorter chains lead to the formation of intercalated nanocomposites.

The cation-exchange process of linear alkylammonium ions is described in Fig. 2.2. Maharaphan et al. [45] modified sodium activated montmorillonite clay using dodecylamine. Dodecylamine in concentrated hydrochloric acid can form dodecylamine hydrochloride, ($CH_3(CH_2)_{11}NH_3$.HCl), which can then be ionized to become the dodecylammonium ion (Equation 2.2). These dodecylammonium ions are exchanged with sodium ions in montmorillonite and form dodecylamine-montmorillonite (DMMT) which is organophilic clay (Equation 2.3). Chemical modification alters the nature of montmorillonite from a pure inorganic to an organic-

like matter or from a hydrophilic to a hydrophobic matter due to the long tail of 12 carbons in dodecylamine [45].

$$\begin{aligned} CH_3(CH_2)_{11} - NH_2 + HCl \quad &\rightarrow \quad CH_3(CH_2)_{11} - NH_2.HCl \\ &\rightarrow \quad CH_3(CH_2)_{11} - NH_3^+ + Cl^- \end{aligned} \qquad (2.2)$$

Cation exchange

$$Clay - Na \xrightarrow{CH_3(CH_2)_{11} - NH_3^+} Clay - NH_3^+(CH_2)_{11}CH_3 + Na^+ \qquad (2.3)$$

Where

$Clay - Na^+$: Sodium montmorillonite

$CH_3(CH_2)_{11}NH_3^+$: Dodecylamine

$Clay - NH_3^+(CH_2)_{11}CH_3$: Dodecylamine treated montmorillonite

Depending on the layer charge density of the clay, the alkylammonium ions adopt different structures between the clay layers like monolayers, bilayers, pseudotrimolecular layers, and paraffin type monolayers as shown in Fig. 2.3. Fig. 2.2 shows that, the alkyl ammonium ions adopt a paraffin type structure (clay with high layer charge density) and the spacing between the clay layers increases by about 10 Å. Alkylammonium ions permit to lower the surface energy of the clay so that organic species with different polarities can get intercalated between the clay layers.

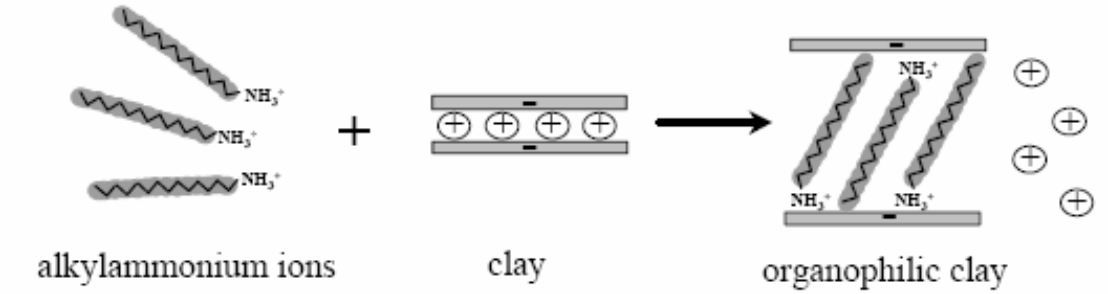

Fig. 2.2: Cation-exchange process between alkylammonium ions and cations initially intercalated [45].

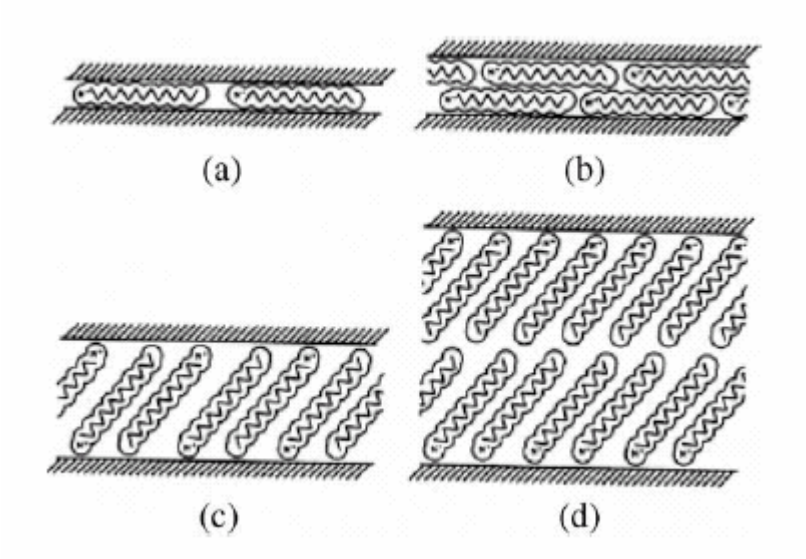

Fig. 2.3 Structure and properties of organically modified clay.
(a) monolayers, (b) bilayers, (c) pseudotrimolecular layers,
(d) paraffin type monolayers [42]

(c) Silanes

Silanes have been used as a compatibilizing agent in the preparation of unsaturated polyester-clay nanocomposites [46]. Silane coupling agents are a family of organo-silicon monomers, which are characterized by the formula R-SiX_3, where R is an organo-functional group attached to silicon in a hydrolytically stable manner and X designates hydrolysable groups, which are converted to silanol groups on hydrolysis. Silane coupling agents interact with "receptive" inorganic surfaces forming tenacious bonds at the interface. These receptive inorganic surfaces are characterized by the presence of hydroxyl groups (OH) attached principally to silicon and aluminum that are particularly favorable for bonding with silanes. In the clay, hydroxyl groups are possibly present on the surface of the layers but also particularly on their edges. The silane coupling agent is first converted to a reactive silanol form by hydrolysis, which

then reacts with hydroxyl groups present on the inorganic surface. The type of bond (oxano or hydrogen) formed during this treatment is still not clearly established.

2.4. STRUCTURE AND PROPERTIES OF ORGANICALLY MODIFIED CLAY (OMC)

The physical mixture of a polymer and clay may not form a nanocomposite. This situation is analogous to polymer blends, and in most cases separation into discrete phases takes place. In immiscible systems, which typically correspond to the more conventionally filled polymers, the poor physical interaction between the organic and the inorganic components leads to poor mechanical and thermal properties. In contrast, strong interactions between the polymer and the organo modified clay in CP nanocomposites leads to the dispersion of organic and inorganic phases at nanometer level. As a result, nanocomposites exhibit unique properties not shown by their micro counterparts or conventionally filled polymers [10-14].

Alkylammonium or alkylphosphonium cations in the organomodified clays lower the surface energy of the inorganic host and improve the wetting characteristics of the polymer matrix, and result in a larger interlayer spacing. Additionally, the alkylammonium or alkylphosphonium cations can provide functional groups that can react with the polymer matrix, or in some cases initiate the polymerization of monomers to improve the strength of the interface between the inorganic and the polymer matrix [35, 47].

Traditional structural characterization to determine the orientation and arrangement of the alkyl chain was performed using wide-angle x-ray diffraction (WAXD). Depending on the packing density, temperature, and alkyl chain length, the chains were thought to lie either parallel to the silicate layers forming mono or bilayers, or radiate away from the silicate layers forming mono or bimolecular arrangements [42].

However, these idealized structures have been shown to be unrealistic using FTIR experiments [48]. Vaia et al. [48] showed that the alkyl chains can vary from liquid-like to solid-like, with the liquid like structure dominating as the interlayer density or chain length decreases, or as the temperature increases. This occurs because of the relatively small energy differences between the trans and gauche conformers. In addition, for longer chain surfactants, the surfactants in the organo-modified clay can show thermal transition akin to melting or liquid-crystalline to liquid-like transitions upon heating.

2.5. TYPES OF CLAY-POLYMER NANOCOMPOSITES

In general, clays have silicate layers of thickness 1 nm and high aspect ratio (e.g. 10-1000). A few weight percent of clay that are properly dispersed throughout the polymer matrix creates much higher surface area for clay/polymer interaction as compared to conventional composites. Depending on the strength of interfacial interactions between the polymer matrix and clay (modified or unmodified), three different types of CP nanocomposites are thermodynamically achievable (Fig. 2.4).

Fig. 2.4 Types of clay-polymer nanocomposites [49]

I. Intercalated nanocomposites: in intercalated nanocomposites, the insertion of a polymer matrix into the inter gallery spacing of clay occurs in a regular crystallographic fashion, regardless of the clay to polymer ratio. Intercalated nanocomposites normally have interlayer of few molecular layers of polymer

in between the layers. Properties of the composites typically resemble those of ceramic materials.

II. Flocculated nanocomposites: conceptually this is the same as intercalated nanocomposites. However, silicate layers of clay are some times flocculated due to hydroxylated edge–edge interaction.

III. Exfoliated nanocomposites: the individual clay layers are separated in a continuous polymer matrix, and the average distance depends on clay loading. Usually, the clay content of an exfoliated nanocomposite is much lower than that of an intercalated nanocomposite.

2.6. TECHNIQUES FOR CHARACTERIZATION OF NANOCOMPOSITES

Generally, the structure of nanocomposites has typically been established using Wide Angle X-ray Diffraction (WAXD) analysis and Transmission Electron Microscopic (TEM) observation. Due to its easiness and availability, WAXD is most commonly used to probe the nanocomposite structure [11-14] and occasionally to study the kinetics of the polymer melt intercalation [50]. By monitoring the position, shape, and intensity of the basal reflections from the distributed silicate layers, the nanocomposite structure (intercalated or exfoliated) may be identified. For example, in an exfoliated nanocomposite, the extensive layer separation associated with the delamination of the silicate layers in the polymer matrix results in the eventual disappearance of any coherent X-ray diffraction from the distributed silicate layers. On the other hand, for intercalated nanocomposites, the finite layer expansion associated with the polymer intercalation results in the appearance of a new basal reflection corresponding to the larger gallery height. Although WAXD offers a convenient method to determine the interlayer spacing of the silicate layers in the

clay, and in the intercalated nanocomposites (within 1–4 nm), little can be said about the spatial distribution of the silicate layers or any structural non-homogeneities in nanocomposites. Additionally, some clays initially do not exhibit well-defined basal reflections. Thus, peak broadening and decrease in intensity are very difficult to study systematically. Therefore, conclusions concerning the mechanism of nanocomposites formation and their structure based solely on WAXD patterns are only tentative. On the other hand, TEM allows a qualitative understanding of the internal structure, spatial distribution of the various phases, and views of the defective structure through direct visualization. However, special care must be exercised to guarantee a representative cross-section of the sample. The WAXD patterns of three different types of nanocomposites are presented in Fig. 2.5. However, TEM is time-intensive, and only gives qualitative information on the sample as a whole, while low-angle peaks in WAXD allow quantification of changes in layer spacing. Typically, when inter-layer spacing exceed 6–7 nm in intercalated nanocomposites or when the inter layers become relatively disordered in exfoliated nanocomposites, associated WAXD features weaken to the point of not being useful.

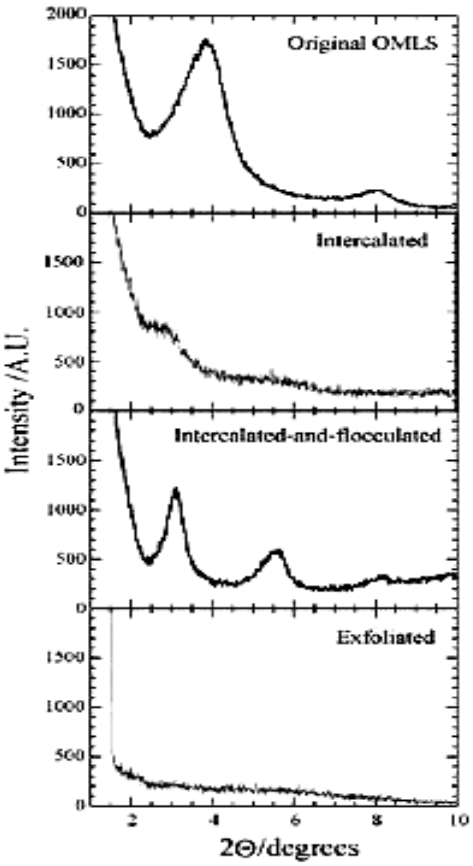

Fig. 2.5: WAXD pattern of different types of clay-polymer nanocomposites [51].

2.7. PREPARATIVE METHODS OF NANOCOMPOSITES

Intercalation of polymers in the intergallery spacing of clay has proven to be a successful approach to prepare CP nanocomposites. The preparative methods are divided into three main groups according to the starting materials and processing techniques.

2.7.1. Intercalation of Polymer or Pre-polymer from Solution

Water-soluble polymers, such as polyethylene oxide [52], polyvinyl acetate [41], polyvinylpyrollidone [53], and polyethylene vinylacetate [54], have been intercalated into the clay galleries using this method. Examples of using non-aqueous solvents are

nanocomposites of polycaprolactone [55] and polylactic acid [56] in chloroform as a co-solvent and high-density polyethylene with xylene and benzonitrile [57]. Nematic liquid crystal CP nanocomposites have also been prepared using this method in various organic solvents, such as toluene and dimethylformamide [58]. The thermodynamics involved in this method are described below. For the overall process, in which polymer is exchanged with the previously intercalated solvent in the gallery, a negative variation in the Gibbs free energy is required. The driving force for the polymer intercalation into the intergallery spacing of clay from solution is the entropy gained by desorption of solvent molecules, which compensates for the decreased entropy of the confined, intercalated chains [27]. Using this method, intercalation only occurs for certain polymer/solvent pairs. This method is good for the intercalation of polymers with little or no polarity into layered structures and facilitates production of thin films with polymer-oriented clay intercalated layers. However, from a commercial point of view, this method involves the copious use of organic solvents, which usually is not environment-friendly and economically prohibitive.

2.7.2. In-situ Intercalative Polymerization Method

Clay-polymer nanocomposites based on epoxy [44], unsaturated polyester [46], polyurethanes [59] and polyethylene terephthalate [60] have been prepared by this method.

In this method, the clay is swollen within the liquid monomer or a monomer solution so the polymer formation can occur between the intercalated sheets. Polymerization can be initiated either by heat or radiation, by the diffusion of a suitable initiator, or by an organic initiator or catalyst fixed through cation exchange inside the interlayer before the swelling step. This method is capable of producing well-exfoliated

nanocomposites and has been applied to a wide range of polymer systems. This technology is suitable for raw polymer manufacturers to produce clay/polymer nanocomposites in polymer synthetic processes and also particularly useful for thermosetting polymers.

2.7.3. Melt Intercalation

Recently, the melt intercalation technique has become the standard for the preparation of CP nanocomposites. During polymer intercalation from solution, a relatively large number of solvent molecules have to be desorbed from the host to accommodate the incoming polymer chains. The desorbed solvent molecules gain one translational degree of freedom, and the resulting entropic gain compensates for the decrease in conformational entropy of the confined polymer chains. Therefore, there are many advantages to direct melt intercalation over solution intercalation. For example, direct melt intercalation is highly specific for the polymer, leading to new hybrids that were previously inaccessible. In addition, the absence of a solvent makes direct melt intercalation an environmentally sound, and an economically favorable method for industries.

2.8. PROPERTIES OF POLYMER CLAY NANOCOMPOSITES

Nanocomposites consisting of a polymer and clay (modified or not) frequently exhibit remarkably improved mechanical and physical properties when compared to those of pristine polymers. Improvement includes higher modulus, increased strength and heat resistance, decreased gas permeability and flammability, and increased biodegradability of biodegradable polymers. The main reason for these improved properties in nanocomposites is the stronger interfacial interaction between the matrix and silicate layers of clay, compared to conventional filler-reinforced systems. Toyota

researchers [36] have reported that delaminated clay-nylon 6 nanocomposites show dramatic improvements in tensile properties. Lan and Pinnavaia [61] have reported more than a ten-fold increase in strength and modulus in a rubbery epoxy matrix with only 15 wt.% (7.5 vol %) of delaminated organoclay. This short review of the tensile properties of clay-polymer nanocomposite suggests that the performance of nanocomposites is related to the degree of delamination of the clay in the polymer matrix that increases the interaction between the clay layers and the polymer. Shi et al. [62] proposed interfacial effects where the direct binding (adsorption) of the polymer to the clay layers would be the dominant factor. Usuki et al. [63] also suggested that the strong ionic interaction between polyamide 6 and silicate layers could generate some crystallinity at the interface, explaining part of the reinforcement effect. Kojima et al. [64] described a concept, where the improvement of tensile modulus in clay-nylon 6 nanocomposites was due to the presence of a constrained region where the polymer chains have a restricted mobility. Fornes et al. [65] reported that the modulus of the nylon 6 is increased much more rapidly by addition of clay than by glass fibers. Specifically, doubling the modulus requires approximately 6.5 per cent by weight of clay whereas the amount of glass fibers required to achieve this value is almost three times. Such mechanical property improvement has resulted in use of nanocomposite materials in numerous applications such as automotive and general / industrial applications. Clays are believed to increase the barrier properties by creating a tortuous path (Fig. 2.6) that retards the progress of the gas molecules through the polymer matrix. The direct benefit of the formation of such a path is clearly observed in clay-polyimide nanocomposites from the dramatically improved barrier properties with a simultaneous decrease in the thermal expansion coefficient [66-68]. The clay-polyimide nanocomposites with a small fraction of OMC exhibited

reduction in the permeability of small gases, e.g. O_2, H_2O, He, CO_2, and ethyl acetate vapors [67]. For example, at 2 wt.% clay loading, the permeability coefficient of water vapor had decreased ten-fold with synthetic mica relative to pristine polyimide. By comparing nanocomposites made with clays having silicate platelets of various aspect ratios, the permeability was seen to decrease with increasing aspect ratio. Such excellent barrier characteristics have resulted in considerable interest in nanoclay composites in food packaging applications.

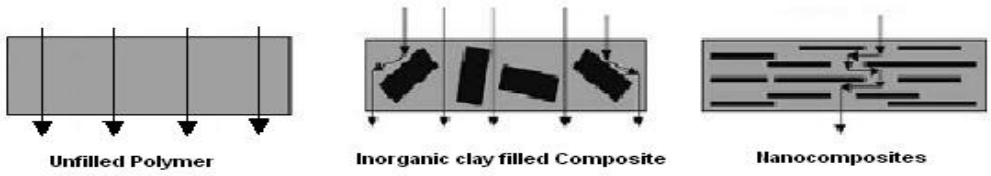

Fig. 2.6 Schematic of mass flow in (a) pure polymer, (b) inorganic clay filled composites and (c) nanocomposites structures [67].

Specific examples include packaging for processed meats, cheese, confectionery, cereals and boil-in-the-bag foods [69], extrusion-coating applications in association with paperboard for fruit juice and dairy products, and beer, and carbonated drinks bottles manufactured by co-extrusion process [9]. The use of nanocomposite formulations would be expected to enhance the shelf life considerably of many types of food [70].

Honeywell [9] have also been active in developing a combined active/passive oxygen barrier system from nylon 6 materials. Passive barrier characteristics are provided by nanoclay particles incorporated through melt processing techniques whilst the active contribution comes from an oxygen-scavenging ingredient. Oxygen transmission results reveal substantial benefits provided by nanoclay incorporation in comparison to the base polymer (approximately 15-20% of the bulk polymer value). The

increased torturosity provided by the nanoclay particles essentially slows transmission of oxygen through the composite and drives molecules to the active scavenging species resulting in near zero oxygen transmission for a considerable period of time.

In 1976 Unitika Ltd in Japan, first presented the potential flame retardant properties of clay-nylon nanocomposites [71]. In 1997 Gilman et al. [21] reported detailed investigations on flame retardant properties of clay-nylon 6 nanocomposite and subsequently they chose various types of nanocomposite materials and found similar reductions in flammability [24]. Recently, Gilman reviewed the flame retardant properties of nanocomposites in detail [22]. According to the authors, the MMT must be nanodispersed to affect the flammability of the nanocomposites, however, the clay need not be completely delaminated. In general, the flame retardant mechanism involves the formation of a high-performance carbonaceous-silicate char, which builds up on the surface during burning. This insulates the underlying material and slows the mass loss rate of decomposition products.

Heat distortion temperature (HDT) of a polymeric material is an index of heat resistance towards applied load. Most of the nanocomposite studies report HDT as a function of clay content, characterized by the procedure given in ASTM D-648. Kojima et al. [64] first showed that the HDT of pure nylon increases up to 90.8ºC after nanocomposite preparation with OMC. Further work carried by them on nylon 6/montmorillonite (MMT) nanocomposites reports the influence of clay content on HDT. In nylon 6/MMT nanocomposites, there is a marked increase in HDT from 65.8ºC for the neat nylon 6 to 152.8ºC for 4.7 wt.% nanocomposite. HDT also depends on the aspect ratio of dispersed clay particles [64]. The nano-dispersion of MMT in the polypropylene matrix [72] and polylactic acid [73] also increased the HDT.

Although silicate layers are microns in lateral size, they are just 1 nm thick. Thus, when single layers are dispersed in a polymer matrix, the resulting nanocomposite is optically clear in visible light. Traditional composites tend to be largely opaque because of light scattering by the particles or fibers embedded within the continuous phase. In nanocomposites, the domain sizes are reduced to a level such that true "molecular composites" are formed. As a result of this intimate mixing, these composites are often highly transparent, a property which renders them amenable to applications outside the boundaries of traditional composites [74, 75]

2.9. MATRIX MATERIAL FOR NANOCOMPOSITES

Nylon 6 was the first matrix material used for the preparation of clay polymer nanocomposites by Toyota researchers [36]. Findings of Toyota researchers made it possible to produce clay-polymer nanocomposites based on other thermoplastic and thermoset polymer systems. The thermoplastics include nylon, polyethylene terepthalate, polyethylene (high density & low density), polypropylene, polyvinyl chloride, polyetheretherketone, thermoplastic polyurethane, etc. The commonly used thermoset polymers for nanocomposite preparation are unsaturated polyester resins, epoxy resins, polyurethane, urea formaldehyde, silicones, etc.

2.10. POLYPROPYLENE

Polyolefins are responsible for the production of approximately 84 billion kilograms of thermoplastic per year or about 50% of the total worldwide polymer industry production. Polypropylene (PP) accounts for approximately 20% of polyolefin production or 34 billion kilograms per year production. Therefore, polypropylene is one of the most widely used thermoplastics, not only because of its balance of physical and mechanical properties, but also due to its environmental friendliness

such as recyclability and low cost [76]. Polypropylene has an excellent combination of low density, high stiffness and toughness and heat distortion temperature above 100℃ which provides it with an extraordinary versatility of properties and applications. Polypropylene is used in several applications such as automotive components, laboratory equipment, plastic parts, food packaging, textiles, and reusable containers. PP has good tensile strength, a superior working temperature but lower impact strength compared to other low or high density thermoplastics. Polypropylene possesses excellent resistance to organic solvents, degreasing agents and electrolytic attack. It is light in weight, resistant to staining, and has a low moisture absorption rate. PP is a tough, heat-resistant, and semi-rigid material, ideal for the transfer of hot liquids or gases. PP is therefore used in vacuum systems where higher heats and pressures are encountered. It also has excellent acid and alkali resistance. Polypropylene can be easily fabricated using hot gas welded, spin welded, fusion & butt welded. PP can also be machined with wood or metal working tools, vacuum formed or ultra-sonic sealed. Innovative catalyst and process technologies have significantly simplified its production, resulting in the minimization of catalyst residues, waxy byproducts and low stereoregularity components, by the use of high activity and highly stereoselective catalysts, such as Ziegler-Natta and metallocene catalysts.

2.11. PHYSICAL AND CHEMICAL PROPERTIES OF POLYPROPYLENE

Most commercial polypropylene has a level of crystallinity intermediate between that of low density polyethylene (LDPE) and high density polyethylene (HDPE). Polypropylenes Young's modulus is also intermediate. Although it is less tough and flexible than LDPE, it is much less brittle than HDPE. This allows polypropylene to

be used as a replacement for engineering plastics, such as acrylonitrile butadiene styrene (ABS). Polypropylene is rigid, stiffer and reasonably economical. It can be made translucent when uncolored but not completely transparent as polystyrene or acrylic. It can also be made opaque and/or have many kinds of colors. Polypropylene has very good resistance to fatigue, so that most plastic living hinges, such as those on flip-top bottles, are made from this material. Very thin sheets of polypropylene are used as a dielectric within certain high performance pulse and low loss RF capacitors. Polypropylene has a melting point of 160 ˚C (320 ˚F). Many plastic items for medical or laboratory use can be made from polypropylene which is autoclavable so that it can withstand the heat in an autoclave. Food containers made from it will not melt in the dishwasher, and do not melt during industrial hot filling processes. For this reason, most plastic tubs for dairy products are polypropylene sealed with aluminum foil (both heat-resistant materials). After the product has cooled, the tubs are often given lids of a cheaper (and less heat-resistant) material, such as LDPE or polystyrene. Such containers provide a good hands-on example of the difference in modulus, since the rubbery (softer, more flexible) feeling of LDPE with respect to PP of the same thickness is readily apparent. Rugged, translucent, reusable plastic containers made in a wide variety of shapes and sizes for consumers from various companies such as Rubbermaid and Sterilite are commonly made of polypropylene, although the lids are often made of somewhat more flexible LDPE so they can snap on to the container to close it. When liquid, powdered, or similar consumer products come in disposable plastic bottles which do not need the improved properties of polypropylene, the containers are often made of slightly more economical polyethylene, although transparent plastics such as polyethylene terephthalate are also used for appearance. Plastic pails, car batteries, wastebaskets, cooler containers, dishes and pitchers are

often made of polypropylene or HDPE, both of which commonly have rather similar appearance, feel, and properties at ambient temperature. MFI (Melt Flow Index) identifies the flow speed of the raw material in the process. It helps to fill the plastic mold during the production process. The higher the MFI increases the weaker the raw material becomes. It also has Copolymer and Random Copolymer. Copolymer helps stiffness of the PP (Polypropylene). Random Copolymer helps transparent look. Copolymer is more expensive than Homopolypropylene. Random Copolymer is even higher than copolymer PP. A rubbery PP can also be made by a specialized synthesis process, as discussed below. Unlike traditional rubber, it can be melted and recycled, making it a thermoplastic elastomer.

2.12. STRUCTURE AND POLYMERIZATION OF POLYPROPYLENE

Structurally, PP is a vinyl polymer, and is similar to polyethylene, with the variation that other carbon atoms in the backbone chain has a methyl group attachment. Polypropylene can be made from the monomer propylene by Ziegler-Natta polymerization and by metallocene catalysis polymerization.

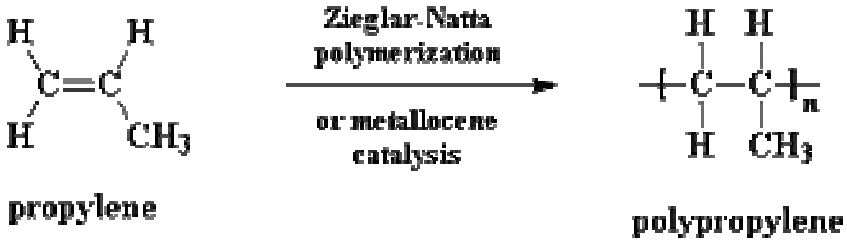

Fig. 2.7: Synthesis of PP using polymerization metallocene catalysis Ziegler-Natta polymerization [77].

Research is being conducted on using metallocene catalysis polymerization to synthesize polypropylene. Polypropylene may be synthesized with different

tacticities. Most polypropylene that is currently used is *isotactic*. This indicates that all the methyl groups are on the same side of the chain.

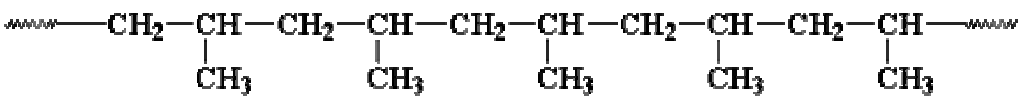

isotactic polypropylene

Fig. 2.8: Structure of Isotactic PP chain [77].

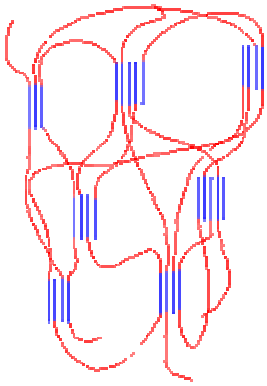

Fig. 2.9: Isotactic polymer PP network [77].

In other processes *atactic* polypropylene is used. *Atactic* PP shows the methyl groups are placed randomly on both sides of the chain.

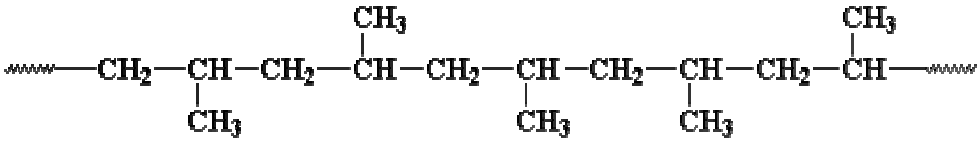

atactic polypropylene

Fig. 2.10: Structure of Atactic PP [77].

However, by using special metallocene catalysts, a polymer that contains blocks of isotactic polypropylene and blocks of atactic polypropylene in the same polymer chain may be synthesized.

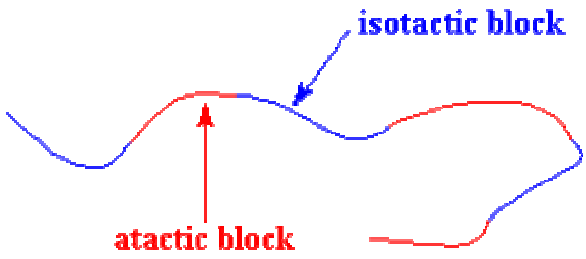

Fig. 2.11: PP polymer chain consisting of isotactic and atactic structures [77].

This polymer is rubbery, and makes a good elastomer. This is due to the formation of crystals from the isotactic blocks. The isotactic blocks are joined to the atactic blocks, the little hard clumps of crystalline isotactic polypropylene are joined together by soft rubbery tethers of atactic polypropylene. Atactic polypropylene would be rubbery without the assistance from the isotactic blocks, but it wouldn't be very strong. The hard isotactic blocks hold the rubbery isotactic material together, to give the material more strength. Most kinds of rubber have to be crosslinked to provide strength, but not polypropylene elastomers. Elastomeric polypropylene, as this copolymer is called, is a kind of thermoplastic elastomer. However, until the research is completed, this type of polypropylene will not be commercially available.

2.13 PROGRESS IN CLAY-POLYPROPYLENE NANOCOMPOSITES

Polypropylene however has some drawbacks. Minimal strength and stiffness, low service temperature and weak barrier properties does not make polypropylene the most ideal thermoplastic to use. To overcome these problems traditional filler materials such as talc and mica have been infused into the PP structure. Although the fillers increased the strength and stiffness, it reduced the impact properties and recyclability. The use of layered silicate materials on the other hand minimises these property trade-offs to some extent but the compatibility of the MMT nanoclays and

PP polymer matrix needs to be improved. Recent advances in polymer clay nanocomposites have yielded two major methods to increase the compatibility between the MMT nanoclays and PP matrix. These are in situ polymerisation and melt intercalation [77]. In the in situ polymerisation method, the clay is used as a catalyst carrier. The propylene monomer intercalates into the interlayer space of the clay and then polymerizes there. The macromolecule chains exfoliate the silicate layers evenly dispersing them in the polymer matrix. In the melt intercalation method, PP and nanoclays are compounded in the melt to form nanocomposites. As the hydrophilic clay is incompatible with polypropylene, compatibilisation between the clay and PP is necessary to form stable PP nanocomposites. This can be achieved via two synthetic routes. In the first route, the clay can be organically modified by the use of a semi-fluorinated surfactant. If the semi-fluorinated surfactant is used judiciously the resulting organoclay will promote PP/clay miscibility effectively [78]. The second route is to use a compatibiliser, such as maleic anhydride grafted PP (PP-MAH) [79, 80]. The clay is melt compounded with the more polar compatibiliser to form an intercalated master batch. The master batch is then compounded with the neat PP to form the PP nanocomposite. In this way, the PP-MAH pretreated OMMT is dispersed uniformly in the PP matrix.

Manias et al. [78] achieved clay polypropylene nanocomposite formation in different ways either by using functionalised polypropylenes and common organo-montmorillonites, or by using neat/unmodified polypropylene and a semifluorinated organic modification for silicates. These hybrids can be formed by solventless melt intercalation or extrusion technique. These techniques resulted in the formation of nanocomposites coexisting with intercalated and exfoliated structures. These nanocomposites show significant improvement in tensile properties, thermal

properties (heat deflection temperature, flame retardancy), barrier properties and scratch resistance when the clay content is less than 6 wt. %.

Lei et al. [81] reported the effect of clay chemistry on processing and properties of the polypropylene nanocomposites. They produced the nanocomposites using different montmorillonite clays like Southern Clays cloisite Na-MMT, 15A, 20A, 30B, and NANOCOR 130E, 131PS. They found that addition of nanoclay in the polypropylene shows improvement in crystallization temperature indicating the nucleating effect of the nanoclays in the crystallization of PP. The extent of crystallization temperature (T_c), varied slightly with the types of clay. However on the other hand the melting temperature of the polypropylene decreases on addition of organoclay. They reported that the introduction of low molecular weight surface modifiers in the clays leads to the decrease in melting temperature. The addition of nanoclay also shows better improvement in storage modulus and softening temperature.

Bertini et al. [82] reported that the maleic anhydride grafted PP (PP-MAH) infused with montmorillonite nanoclays showed widespread exfoliated structures than the isotactic polypropylene homopolymers. The thermal stability of PP-MAH improved in air temperature due the physical barrier effect of the silicate layers. They also reported that the degree of exfoliation plays an important role in improvement of PP barrier properties.

Ding et al. [83] produced clay polypropylene nanocomposites using highly effective PP solid phase graft as compatibiliser and they reported that the property of polypropylene was maintained as very low amount of pp graft was used. They also reported that, addition of organo-montmorillonite (OMMT) significantly improves the impact strength and thermal stability of PP characterized by the initial decomposition

temperature. They also showed that crystallization temperature of PP increased significantly with the infusion of nanoclays.

Peter et al. [84] used octodecylamine treated montmorillonite and PP-g-maleic anhydride compatibiliser to produce clay-polypropylene nanocomposites by in-situ intercalation technique. They reported that the morphology of the samples after extrusion was not stable and they also reported that annealing the samples at 220 ˚C for 200 minutes leads to further exfoliation and self assembly into skeleton structure of layered silicate at the same time. That is the thermal treatment of the nanocomposite samples during processing has the tendency to dramatically change the morphology of nanocomposites.

Qin et al. [85] produced clay polypropylene nanocomposites using melt processing technique. They reported that addition of organo-modified MMT in nanocomposites causes a ceramic like compact char during combustion test and this is an important factor for flame retardancy of polymer/layered silicate composites. The addition of MMT also increases the decomposition temperature of PP. they reported that the improvement was not only due to the barrier effects of the MMT and also due to the physico-chemical adsorption of the volatile degradation products on the silicates.

Galgali et al. [86] used a micromechanical model to predict the effect of clay orientation on the tensile modulus PP-cloisite 20A nanocomposites. They found that the model predicted the values of the modulus semi-quantitatively and can thus provide a reasonable engineering estimate for the modulus of polymer nanoclay composites from independently measured orientation of the clay**.**

In this study we wish to enhance the mechanical properties of polypropylene. We aim to infuse low weight percentages of organically modified MMT nanoclays (Cloisite®15A) into a polypropylene thermoplastic by melt blending. In contrast to

other organoclays used presently the use of Closite®15A nanoclays will provide increased compatibility between the MMT layered silicates and PP polymer matrix. This increased compatibility will result in the synthesis of polymer and layered silicate composite structures with at least one dimension in the nanoscale. This in turn will result in polypropylene having improved properties. To verify this, the nano-infused PP structures have been subjected to quasi-static mechanical tests to determine any improvement in properties. TEM studies are used to characterise the morphology of the nanocomposite structures while SEM will be used to complete fracture surface analysis. We present this work on the morphology and mechanical properties of the polypropylene-closite®15A interface in an attempt to better understand the unique behaviour of polymer nanocomposites.

2.14 TRIBOLOGICAL PROPERTIES OF NANOCOMPOSITE

Chang et al. [87] investigated the tribological performances of epoxy-based composites, filled with short carbon fibre, graphite, polytetrafluroethylene (PTFE), and nano-TiO_2 in different proportions and combinations. They examined the patterns of coefficient of friction (C.O.F), wear resistance and temperature generated at contact point by a pin-on-disc apparatus in a dry sliding condition under different contact pressures, and sliding velocities. They have reported that the addition of nano-TiO_2 could apparently reduce the frictional coefficient, and consequently reduce the contact temperature of fiber-reinforced epoxy composites. The wear resistance of the composites was significantly high, especially at extreme wear conditions, i.e. high contact pressures and sliding velocities. They have reported that the reduction in C.O.F might be due to the nanoscale polishing effect. Similar observation has been reported by Zhang et al. [88]. Zhang et al. [89] have also reported that, with the

appropriate size, hardness, and volume content, the nanoparticles could polish the counterpart surface to a very fine scale and results in reduction of frictional coefficient and the related shear stress. Chang et al. [87] suggested that the nano and micro scale rolling effect under certain wear conditions could also reduce both the frictional coefficient and the wear rate considerably.

Wang et al. [90] investigated the friction and wear properties of nanometer SiO_2 filled-polyetheretherketone (PEEK) composite blocks by running a plain carbon steel (AISI 1045 steel) ring against the composite block. They have reported that the nanometer SiO_2 filled-PEEK exhibited considerably lower friction coefficient and wear rate in comparison with pure PEEK. The lowest wear rate was obtained with the composite containing 7.5 wt. % SiO_2. They have also reported that the friction coefficient decreases with increase in load for nanometer SiO_2 filled-PEEK composite. The formation of thin, uniform and tenacious transfer film on the counterpart steel surface during the friction process contributes in decreasing friction coefficient and wear rate of the filled PEEK composites.

Wang et al. [91] investigated the wear tracks and found that plucked and ploughed marks appeared on the wear surface of pure PEEK and scuffing of wear scar is found on nano ZrO_2 filled PEEK. They have reported that, the improvement in the tribological behavior of nanometer ZrO_2-filled PEEK composite is closely related to the improved characteristics of the worn surfaces.

Wang et al. [92] investigated the friction and wear behavior of PEEK filled with nanometer SiC. They have reported that the nanometer SiC has effectively reduced the friction coefficient of the PEEK and also reported that 2.5 wt.% SiC to 10 wt.% SiC has effectively reduced the wear of the PEEK. For the nanometer SiC filled PEEK, a thin tenacious transfer film is formed on the steel counter face. They have

also reported that the incorporated nano SiC act as load carrier, and also increases the adhesive strength of the transfer film through chemical reaction with steel substrate, and thereby avoids the direct contact of SiC filled PEEK with the counter face resulting in improved wear resistance. They have also reported that at high SiC content (>10 wt.%) the friction coefficient is increased due to the weakening of transfer film.

Wang et al. [93] investigated the wear properties of nanometer Si_3N_4 filled polyetheretherketone (PEEK) composite blocks with different filler proportions, prepared by compression molding. Their friction and wear properties under distilled water lubrication, as well as under ambient dry conditions, were investigated by running a plain carbon steel (AISI 1045 steel) ring against the PEEK composite block. They have reported that the distilled water medium has brought down the C.O.F of the filled composite with large reduction in wear resistance and the dominant wear mechanism of the filled PEEK was severe abrasive wear with surface fracture.

Sawyer et al. [94] investigated the effect of nano Al_2O_3 on the friction and wear properties of polytetrafluroethylene (PTFE). They have reported that the nano Al_2O_3 particle addition has increased the wear resistance by 60 %. It has increased the wear resistance monotonically and also no optimum weight fraction of Al_2O_3 was found.

The sliding wear performance of epoxy composites filled with nano-sized Al_2O_3 particles was investigated by Shi et al. [95]. They have reported that the frictional coefficient and wear rate of epoxy can be reduced at rather low concentration of nano-Al_2O_3, and also reported that the pretreatment by silane coupling agent also favors the improvement in wear resistance properties.

From the detailed literature survey, it was found that the incorporation of nano particles has improved the wear resistance and friction coefficient of polymer matrix tremendously. Polypropylene-nanoclay nanocomposites find application in various fields, and so it will be useful if detailed work is conducted on the tribological properties of polypropylene-nanoclay nanocomposites.

2.15 MOTIVATION

The infusion of nanoclays into the polymer matrices of thermoplastics and thermosets have improved the polymers mechanically and thermally with increased barrier properties. Therefore, the motivation of this work is to better understand the influence that organo-modified clays has on the physical properties and morphological structure of polypropylene on both micro and nano level.

2.16 SCOPE OF THE WORK

Extensive research is in progression to find lighter materials with higher strength, greater stiffness, better reliability and recyclability. This demand had led to the development of a new class of materials called polymer-clay nanocomposites. These nanocomposite materials offer a combination of higher strength, and modulus better than many of conventionally filled composites. Low strength and stiffness, low service temperature and weak barrier properties does not make polypropylene the most ideal thermoplastic to use. Hence, the use of nanocomposite materials offers a high strength-to-weight ratio, as well as high modulus-to-weight ratio render these materials superior to conventional composite materials. At nanoclay loading levels of 2–7 wt%, they offer similar performance to conventional polymeric composites with 30–50 wt% of reinforcing material. The high filler loading in the latter materials causes undesirable increase of density, hence heavy parts, decreased melt flow and

increased brittleness. The classical composites are opaque with often poor surface finish. These problems are absent in polymer nanocomposites (PNC). Current consumption of PNC is but a few Kton per annum, to increase by 2009 to 500 Kton/y. Cost differential between the neat polypropylene matrix and its PNC is about 10%. Polymer nanocomposites main market is in the transport industries, with growing demand for packaging, appliances, building & construction, electrical & electronic, lawn & garden, power tools, etc. Their advantages range from enhancement of mechanical performance, to reduction of permeability and flammability, improved optical properties, modified magnetic, electric or light-transmitting performance, biocompatibility and thermochromic effects.

2.17 OBJECTIVES OF THE WORK

1. To prepare polypropylene nanocomposites by infusing low weight percentages of organically modified MMT nanoclays (Cloisite®15A) into a polypropylene thermoplastic by melt blending. These organoclays (Closite®15A nanoclays) will provide increased compatibility between the MMT layered silicates and PP polymer matrix.
2. To study mechanical, thermal and physical properties of virgin and infused polypropylene structures.
3. To study the influence of organoclay on the tribological properties of polypropylene nanocomposites.

CHAPTER 3

EXPERIMENTAL METHODS

3.1. INTRODUCTION

This section deals with the procedures used in the synthesis of polypropylene nanocomposites. Further discussions involve the various mechanical test methods and morphological analysis performed on the virgin and nanocomposite specimens.

3.2. MATERIALS

3.2.1 Polypropylene

Polypropylene used as the polymer matrix was obtained from a Durban based company CHEMPRO, in South Africa. The manufacturers data for COSMOPLENE polypropylene is given in table 3.1,

Table 3.1: Properties of COSMOPLENE®Y101E POLYPROPYLENE

ITEM	UNIT	Y101E	ASTM METHOD
Melt Flow Rate	g/10 mins	17	D1238
Density	g/cm^3	0.90	D1505
Tensile Strength at break	kg/cm^3	350	D638
Elongation	%	>600	D638
Flexural Modulus	kg/cm^2	14,000	D790
Izod Impact strength	kg·cm/cm	2.0	D256
Melting Point	°C	165	N/A

3.2.2 Nanoclays

The nanoclay material, Closite 15A were obtained from SOUTHERN CLAYS PRODUCTS, a company based in the United States of America. Cloisite 15A is a natural montmorillonite modified with a quaternary ammonium salt which is off white in colour.

The typical properties of Cloisite 15A is given in table 3.2,

Table 3.2: Properties of Cloisite®15A

Treatment/Properties:	Organic Modifier	Modifier Concentration	% Moisture	% Weight Loss on Ignition
Cloisite® 15A	2M2HT dimethyl, dehydrogenated tallow, quaternary ammonium	125 meq/100g clay	< 2%	43%

Hydrogenated Tallow (~65% C18; ~30% C16; ~5% C14), HT is shown below,

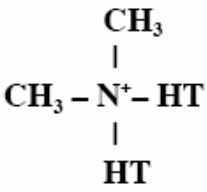

Fig 3.1: Organic structure of Hydrogenated Tallow

The typical dry size properties of Cloisite 15A is given in table 3.3, (microns, by volume),

Table 3.3: Cloisite®15A dry particle sizes

10% less than	50% less than	90% less than
2μm	6μm	13μm

The density of Cloisite 15A is given in table 3.4,

Table 3.4: Density of Cloisite®15A

Loose Bulk, kg/m^3	Packed Bulk, kg/m^3	Density, g/cm^3
172.84	298.58	1.66

3.3 PROCESSING TECHNIQUES

3.3.1 Melt Blending Technique

Nanophased thermoplastic composite structures were prepared by infusion of Cloisite 15A nanoclays into a polypropylene matrix using a mechanical melt blending method. Polypropylene (PP) pellets were heated to its melt temperature in a LABCON HTR2 environmental chamber.

Fig. 3.2: LABCON HTR2 environmental chamber

To avoid thermal shock, the temperature was ramped 10°C/min to a maximum temperature of 170°C. Upon reaching the desired temperature, the material was left in the oven at the set temperature to effect temperature soaking. The temperature was measured using a (TESTO QTA25-T4 PYROMETER) probe with the LACON HTR2 digital display. The plastic surface and chamber temperature was measured accurately within a ± 2°C range thus allowing successful control of temperature ramping.

3.3.2 Screw Extrusion

Single screw extrusion is one of the core operations in polymer processing. The main objective of a single screw extrusion process is to build pressure in the polypropylene polymer melt so that it can be extruded through a die or injected into a mould. Extruders are plasticating machines that convert polymer solids, in pellet or powder form, into molten material as well as building pressure. The REIFFENHAEUSER

screw was used for processing virgin polypropylene panels. The extruder has a 40 mm single rotating screw with a length / diameter ratio (L/D) of 24 and driven by a 7.5 kW motor. The extrusion temperature profile was set to increase to 200 ˚C to melt virgin PP pellets fed to the single barrel from a stainless steel hopper. The molten PP polymer was then injected into an aluminium mould and cast at room temperature.

3.3.3 Moulds

Virgin and nanophased PP structures were obtained by casting the molten polymer. The molten polymer was placed into an aluminium mould with dimensions, 275 ×175 × 10 mm, allowing it to set at room temperature.

(a)

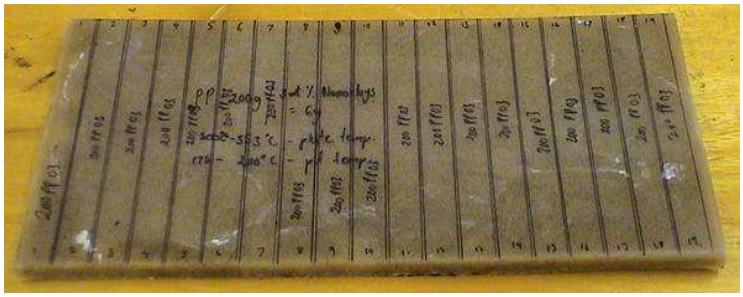

(b)

Fig 3.3: (a) Casting of virgin and nano-infused polymers in aluminium mould.
(b) Cured panel of polypropylene infused with cloisite 15A nanoclay.

3.4 SPECIMEN PREPARATION

3.4.1 Preparation of virgin and PP nano-infused specimens

A very viscous homogenous molten plastic at melt temperature was removed from the environmental chamber and cooled at room temperature to form a virgin panel. A similar technique was employed to manufacture the nanophased structures except the temperature was ramped at 10°C/min to a maximum temperature of 185°C. Cloisite®15A nanoclays measured in specific weight percentages 0.5 wt. %; 1 wt. %; 2wt. %; 3 wt. % and 5 wt. %; were added to separate batches of the molten plastic. The mixtures were vigorously blended using a paddle stirrer for approximately 3 minutes, then cast in moulds and allowed to cure at room temperature. Test coupons were cut from these panels of dimensions, 125 × 13 × 6 mm.

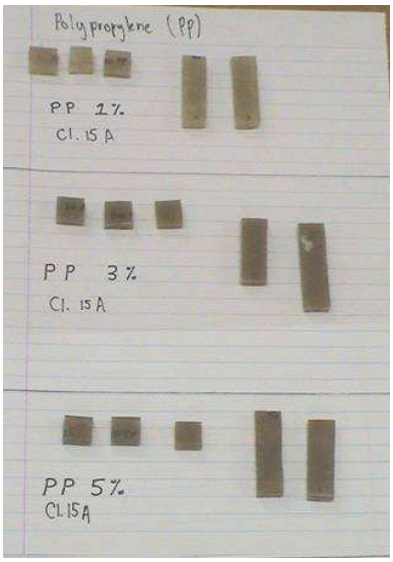

Fig. 3.4: Polypropylene cloisite 15A nanocomposite test specimens

3.5. CHARACTERIZATION

3.5.1 X-ray Diffraction (XRD)

X –Ray diffraction patterns were obtained using a Philips PW1050 diffractometer using monochromated Co-Kά radiation. (λ = 0.1788965 nm, 40 kV, 120 mA) at room temperature. The diffractrograms were scanned from 2.5˚ to 10° (2θ) in steps of 0.02˚ using a scanning rate of 0.5˚/min. X-ray diffractograms were taken on closite 15A clay and polypropylene composites containing 0.5, 1, 2, 3 and 5 wt.% closite 15A nanoclay to confirm the formation of nanocomposites on addition of organo clay. Molten virgin PP and the molten PP nanocomposites structures were allowed to cure at room temperature in the slide templates shown in figure 3.4.

Fig. 3.5: XRD specimens

3.5.2 Transmission Electron Microscopy (TEM)

Polypropylene nanocomposites were analyzed by transmission electron microscopy (TEM) in an effort to characterize the nanoscale dispersion of the layered silicate. Microscopic investigation of selected nanocomposite specimens at the various weight compositions were conducted using a Philips CM120 BioTWIN transmission electron microscope with a 20 to 120 kV operating voltage. The cryo and low dose imaging

TEM has BioTWIN objective lens that gives high contrast and a resolution of 0.34 nm. The microscope is equipped with an energy filter imaging system (Gatan GIF 100) and digital multiscan CCD cameras (Gatan 791). The specimens were prepared using a LKB/Wallac Type 8801 Ultramicrotome with Ultratome III 8802A Control Unit. Ultra thin transverse sections, approximately 80-100 nm in thickness were sliced at room temperature using a diamond knife. The sections were supported by 100 copper mesh grids sputter-coated with 3 nm thick carbon layer.

3.6. QUASI-STATIC MECHANICAL TESTS

All of the following quasi static tests were performed on a minimum of five specimens per test.

3.6.1 Tensile Tests

Tensile tests were performed on virgin PP and the nanocomposite specimens using the LLOYDS Tensile Tester fitted with a 20 kN load cell. The tensile tests were performed at a crosshead speed of 1 mm/min in accordance with the ASTM D3039 standard [96].

3.6.2 Flexural Tests

The flexural tests were used to find the flexural modulus and strength of pristine PP and nano-infused PP specimens. Flexural tests were performed on specimens with dimensions 125 × 13 × 6 mm using a three point bend fixture with a span length of 100 mm. The LLOYDS tensile testing machine was used with a crosshead speed of 1 mm/min to conduct the tests according to the ASTM D790 testing standard.

3.6.3 Vickers Hardness Tests

The Vickers hardness of the virgin and nano-infused polypropylene specimens was determined using a Matsuzawa DMH2 micro-hardness tester. Specimens of dimension 14 ×12 × 6 mm were indented with a 100 gf load in five different sections for a period of 5 seconds. The diagonals of each indentation were measured and the Vickers hardness was automatically computed and read of a digital display.

3.6.4 Impact Testing

The impact tests was used to find the energy absorbed during the fracture of a specimen when subjected to very rapid (impact) loading. Impact tests were performed on the specimens with dimensions, 40 × 13 × 6 mm using a bench scale Izod impact tester. These specimens were tested according to ASTM D256 testing standard [97] to determine the impact strength.

3.6.5 Compression Testing

Compression tests on the nanocomposite specimens were performed using the LLOYDS Tensile Tester fixed with a 20 kN load cell. The compression testing was carried on specimens with dimensions of 15 X 8 X 8 mm.

3.6.6 Scanning Electron Microscopic Studies

Surface scanning studies were conducted using a Philips XL30 Environmental SEM with accelerating voltage 0.2 to 30 kV and magnification 15 to 500 000. The microscope is equipped with a conventional filament emission gun giving a beam spot size of 20 nm and image resolution of 2 nm. Thin transverse sections, approximately 2 to 7 mm in thickness were cut from selected specimens. This analysis was performed on the fracture surface of tensile tested PP nanocomposites.

3.6.7 Fracture Toughness

The stress intensity factor ($\mathbf{K_{IC}}$) and the strain energy release rates ($\mathbf{G_{IC}}$) for neat and nanocomposite specimens were determined by the single-edge notch bending specimen (SENB) in Mode 1. A minimum of three specimens were tested for each weight category of the nano-infused structure. The specimens were prepared in accordance with the ASTM D5045-93 testing standard. Specimens with dimensions 125 × 25 × 6 mm were notched to a depth of 5 mm with a thin saw blade and a grid was plotted on the front view of the specimen to observe the crack propagation. The LLOYDS tensile testing machine fixed with a 20 kN load and fitted with a three-point bend fixture was used to conduct the tests. The critical load (load at which fracture occurs, $\mathbf{P_C}$) was recorded for each specimen. The stress intensity factor ($\mathbf{K_{IC}}$) was determined as follows,

$$K_{IC} = \frac{P_C}{B\sqrt{W}} f\left(\frac{a}{w}\right) \qquad (3.1)$$

where,

K_{IC} = stress intensity factor (MPa.m$^{0.5}$)

P_C = critical load (N)

B = thickness of specimen (m)

W = height of specimen (m)

f(a/w) = correction factor

$$f\left(\frac{a}{w}\right) = \frac{3\frac{S}{W}\sqrt{\frac{a}{W}}}{2\left(1+2\frac{a}{w}\right)\left(1-\frac{a}{w}\right)^{\frac{3}{2}}}\left[1.99 - \frac{a}{w}\left(1-\frac{a}{w}\right)\left\{2.15 - 3.93\left(\frac{a}{w}\right) + 2.7\left(\frac{a}{w}\right)^2\right\}\right] \qquad (3.2)$$

where,

S = span length of the specimen

a = notch depth

w = height of the specimen

The strain energy release rates ($\mathbf{G_{IC}}$) was determined as follows,

$$G_{IC} = \frac{K_{IC}^{\ 2}}{E} \qquad (3.3)$$

where,

G_{IC} = critical strain energy release rate (J/m^2)

E = Youngs Modulus (GPa)

3.6.8 Dynamic Mechanical Analysis

Dynamic mechanical analysis (DMA) was performed using the dynamic mechanical analyzer (TA DMA Q800) in the three point bending mode at a frequency of 10Hz over the temperature range of -60 to 120°C at a heating rate of 2°C/min. The dynamic mechanical analysis was conducted to determine the storage modulus of PP and nanocomposite samples at cryogenic temperature, room temperature and at high temperatures and also the glass transition temperature.

3.6.9 Tribological Testing

Wear tests on virgin and nano infused polypropylene specimens was carried out using locally fabricated tribometer according to ASTM G-99 standard. The tribometer consists of loading disk for load application over square pins. The dimension of the wear test pins is 8 mm square and 20 mm in length. The disc used was brass of surface roughness 0.2 µm. The wear loss of conventional composites, and nanocomposites was determined at a constant contact pressure of 0.15 MPa

and sliding velocity of 0.35 m/s for the sliding distance of 3600 m. Wear tracks of pins was observed using an optical microscope.

CHAPTER 4

RESULTS AND DISCUSSION

4.1 X-RAY CHARACTERIZATION

The basal spacing or d-spacing may be determined using Bragg's equation. This is the distance between basal layers of the MMT molecule.

$$d = \frac{\lambda}{2 \sin \theta} \tag{4.1}$$

XRD is used to calculate this interlayer d-spacing [11]. This may be used to describe the dispersive nature of the layered silicate nanoclays within a polymer matrix [88]. Generally an increased spacing between the basal layers and a hydrophobic, organophilic surface make it more likely for the polymer to enter between the layers of the clay [47]. The XRD pattern of closite 15A and polypropylene infused with 0.5, 1, 2, 3 and 5 wt. % closite 15A is shown in figure 4.1. The graph shows a distinct peak at 2θ value of 3.3° and the corresponding initial intergallery spacing is 31.09 Å. During mixing, the polymer infuses and intercalates between the intergallery spacing of layered silicates and makes the clay layers to move apart. The disappearance of peak indicates the separation of clay layers and the formation of nanocomposites at 0.5 wt.% to 2 wt.% clay loadings. This is confirmed by transmission electron microscopic studies indicating that predominantly exfoliated nanoclay structures have formed in 0.5 wt. % and 1 wt. % nanoclay polypropylene specimens. Polypropylene infused with 2 wt. % nanoclays has more intercalated clay structures.

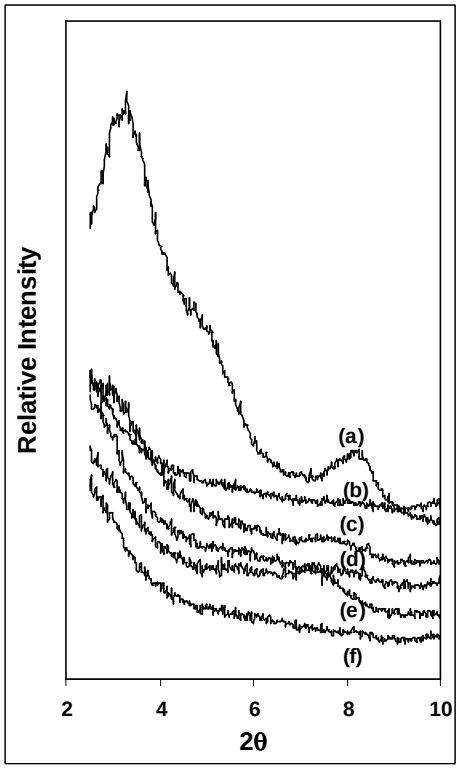

Fig. 4.1: X-ray diffraction pattern of (a) closite 15A and polypropylene with (b) 0.5 wt.% closite 15A, (c) 1 wt.% closite 15A, (d) 2 wt.% closite 15A, (e) 3 wt. % closite 15A and (f) 5 wt.% closite 15A.

4.2 TRANSMISSION ELECTRON MICROSCOPE (TEM) STUDIES

The formation of a nanocomposite involves the break-up and dispersion of the agglomerated stacks of sheets followed by the swelling of the gallery spacing between the sheets by the polymer [98]. The structures are then classified by three indicators. An intercalated nanocomposite structure is formed when the interlayer spacing between the platelets increases to at least 1.5 nm. An exfoliated structure is formed when individual platelets dispersed in the matrix are separated by distances greater than 8.8 nm and the platelets can be orientated, forming short stacks or tactoids [99]. An agglomerated clay structure is formed when no polymer penetrates the interlayer spacing thus forming clustered platelets. These structures are micron sized particles

reminiscent of conventional micro composite filler materials. The following TEM images show these various types of morphologies.

Figure 4.2 shows an image of a polypropylene structure infused with 0.5 wt. % of nanoclays.

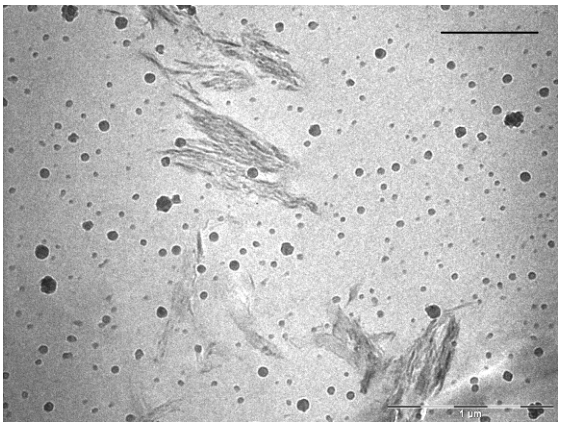

Fig. 4.2: TEM image of PP infused with 0.5 wt. % nanoclays.

In this image various structures can be seen. Darker stacked arrangement of lines and random lines are visible against the lighter background. This suggests that mixed morphologies of exfoliated and intercalated nanostructures have been synthesised. Even at this low weight loading of clay, the stiffness and strength of virgin polypropylene have increased by 60 % and 80 % respectively (section 4.3.1). SEM analysis at this loading shows good dispersion of clays in these structures (section 4.4). Figure 4.3 shows an image of a section of polypropylene infused with 1 wt. % of nanoclays.

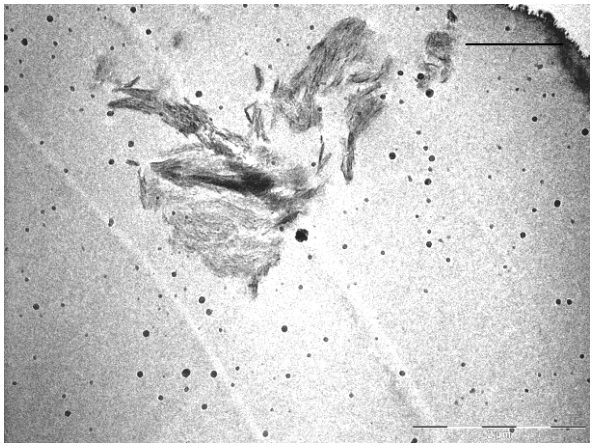

Fig 4.3: TEM image of PP infused with 1 wt. % nanoclays.

Three types of structures may again be seen. Stacked clay tactoids representative of intercalated morphology, random clay platelets representative of exfoliated morphology and large dark structures occurring amongst some of the clay tactoids are visible. Another finding is that the mixed morphologies of intercalated and exfoliated structures are in close proximity of each other. The closeness of these structures suggests that the polymer matrix is becoming increasingly reinforced. This phenomenon explains the increasing modulus and strength properties. This is consistent with findings by Ding et al who stated that organically modified MMT is dispersed or intercalated in a PP matrix on the nanoscale may confine segmental movement of PP macromolecules. Also arrangements like these contribute to reinforcement effects and improvement in flexural and tensile properties. [100]. Figure 4.4 shows an image generated by exploring a section of polypropylene infused with 2 wt. % of nanoclays.

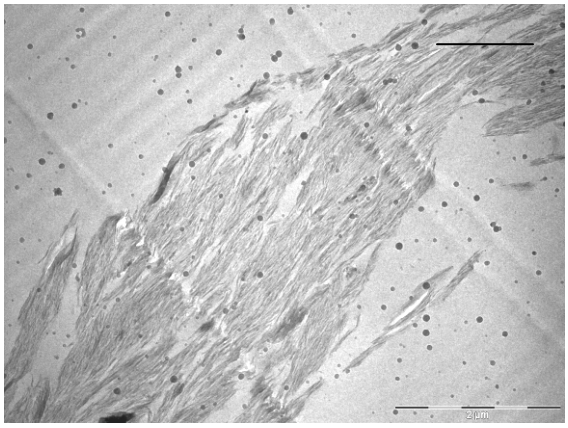

Fig 4.4: TEM image of PP infused with 2 wt. % nanoclays.

The image displays darker lines against the lighter polymer background section. The lines show an ordered stacked arrangement with clearly visible interspaces. This suggests the formation of a tactoid nanoclay structure. The structure consists of 1 nm thick platelets arranged in a stacked formation where the interlayer space between each platelet is occupied by chains of polymer molecules. R. K Bharadwaj et al. showed similar structures where this type of morphology exists [98]. Their nanocomposite structures showed increases in tensile strength at low weight percentage loadings of nanoclay. This arrangement of clay platelets can be associated with that of an intercalated nanocomposite structure. At this clay loading, maximum enhancement in properties occurred. Figure 4.5 shows an image of polypropylene infused with 3 wt. % of nanoclays.

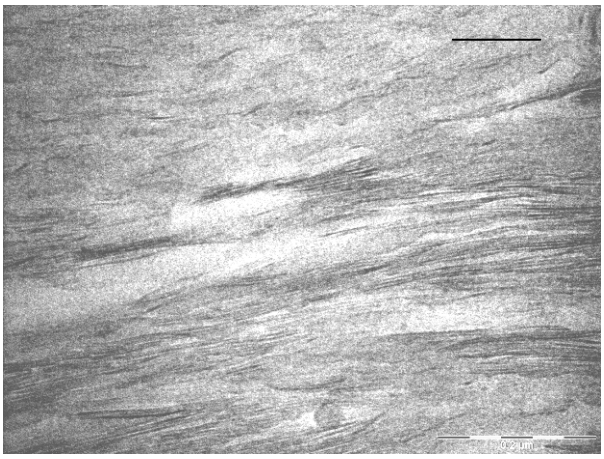

Fig. 4.5: TEM image of polypropylene infused with 3 wt. % nanoclays

A mixed morphology can be distinguished and is described as a highly stacked intercalated structure with some resemblance to an agglomerated clay tactoid. At this clay loading there was a decrease in the mechanical properties however the structure still performed better than virgin PP. This may be attributed to the dual effect of intercalation and agglomeration. Closer examination of the singular dark structure in figure 4.3 reveals the polymer has not been able to penetrate the interlayer between platelets. This particle is micron-sized and is very similar to micro composite structures formed by conventional filler silicates. Ding et al. and Bharadwaj et al. both suggested that these aggregated sites or agglomerations were responsible for diminished properties and brittleness at high clay concentrations. In line with their findings and the TEM images, we suspect that these structures may be responsible for the degradation of mechanical properties at 3 wt. % and 5 wt. % clay loadings. The decrease in properties is also consistent with findings by Yi and Sastry [101]. They stated at low density, most particles are isolated, and therefore smaller clusters dominate. At high density, however, particles are more likely to be interconnected and thus larger clusters dominate [102]. The larger clusters also showed increased

percolation probability at volume fractions larger than the percolation threshold. This verifies that larger clusters, described as clay agglomerates in this study, will form at high volume fractions.

Figure 4.6 shows an image of polypropylene infused with 5 wt. % of nanoclays.

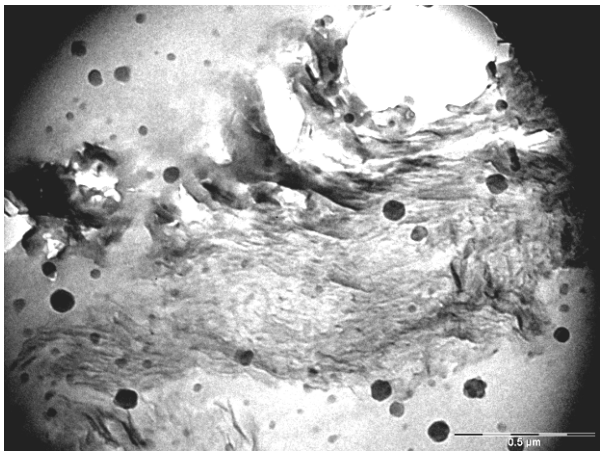

Fig. 4.6: TEM image of polypropylene infused with 5 wt. % nanoclays.

This image represents sites that frequently occurred across this section. Three distinct morphologies are clearly visible. Region A shows areas where arrangements of stacked lines are prevalent. This indicates presence of intercalated morphology. Region B shows areas where darker lines or patches are noticeable. These sites show little penetration by the polymer into the interlayer resulting in agglomerated clay sites. Region C shows the formation of a micro void due to aeration or where micron sized clay agglomerate fell away from the polymer structure during microtome sectioning. Formation of micro voids and clay agglomerates may be the cause for degraded mechanical properties at this clay loading.

4.3 QUASISTATIC MECHANICAL TESTING

4.3.1. Tensile Tests

The tensile test data obtained was used to plot stress-strain curves for the various nanocomposite structures. Figure 4.7 shows the average stress-strain data computed for virgin polypropylene specimens.

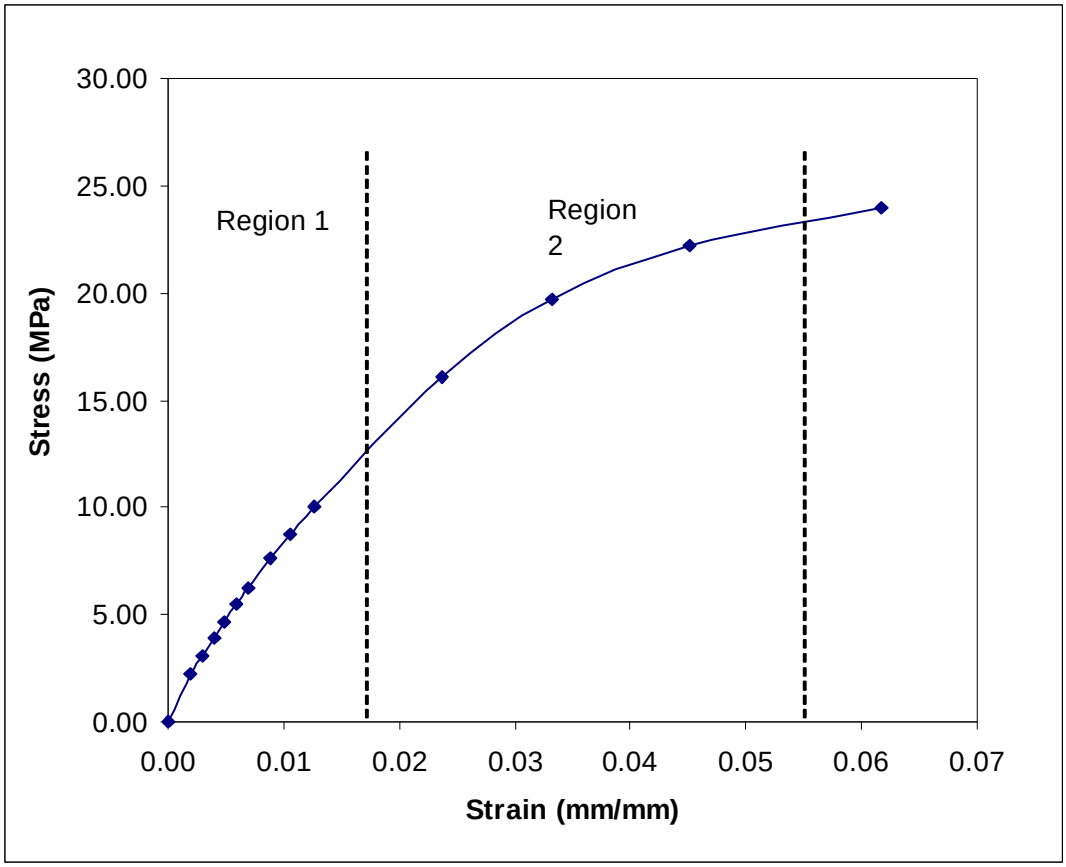

Fig. 4.7: Stress versus strain for virgin polypropylene specimens loaded in tension.

The stress-strain response of neat polypropylene is shown in figure 4.7 and is typical of visco-elastic materials. Two distinct regions can be seen. In region 1, up to approximately 14 MPa the material displays an elastic behaviour, thereafter the graph assumes a non-linear path noticeable in region 2 and is typical of a ductile response. Elastic-plastic failure occurs upon reaching a stress of approximately 23 MPa. The specimens failed with a low audible snap and failure was always within the gauge

length. The fracture was clean with minimal fragmentation and figure 4.8 represents a comparative stress versus strain plot for virgin polypropylene nano-infused specimens.

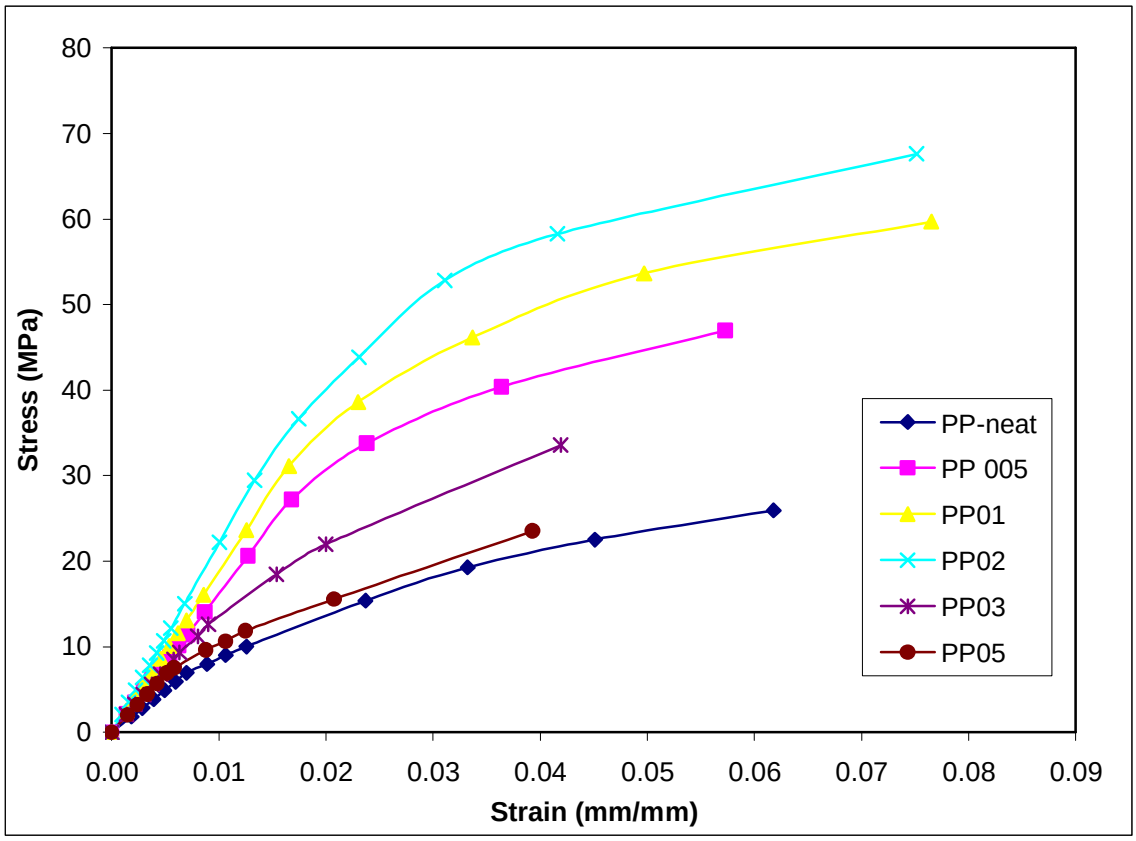

Fig. 4.8: Stress versus strain behaviour of pristine polypropylene and polypropylene nanocomposites infused at various clay weight loadings.

Analysis of the slopes in the elastic region of the plot shows an increase in gradient with increasing clay content. The increase in gradient indicates an increase in the material stiffness with an increase in nanoclay loading up to 2 wt. %. Nanocomposite structures containing 3 wt. % and 5 wt. % clay concentrations showed slopes of lower gradient than 0.5 wt. % specimens but were still steeper than virgin specimens. This suggests that the stiffness increased with increasing clay concentration up to 2 wt. % and then decreased for clay concentrations greater than 2 wt. %. Figure 4.9 shows the elastic modulus and tensile strength as a function of clay concentration.

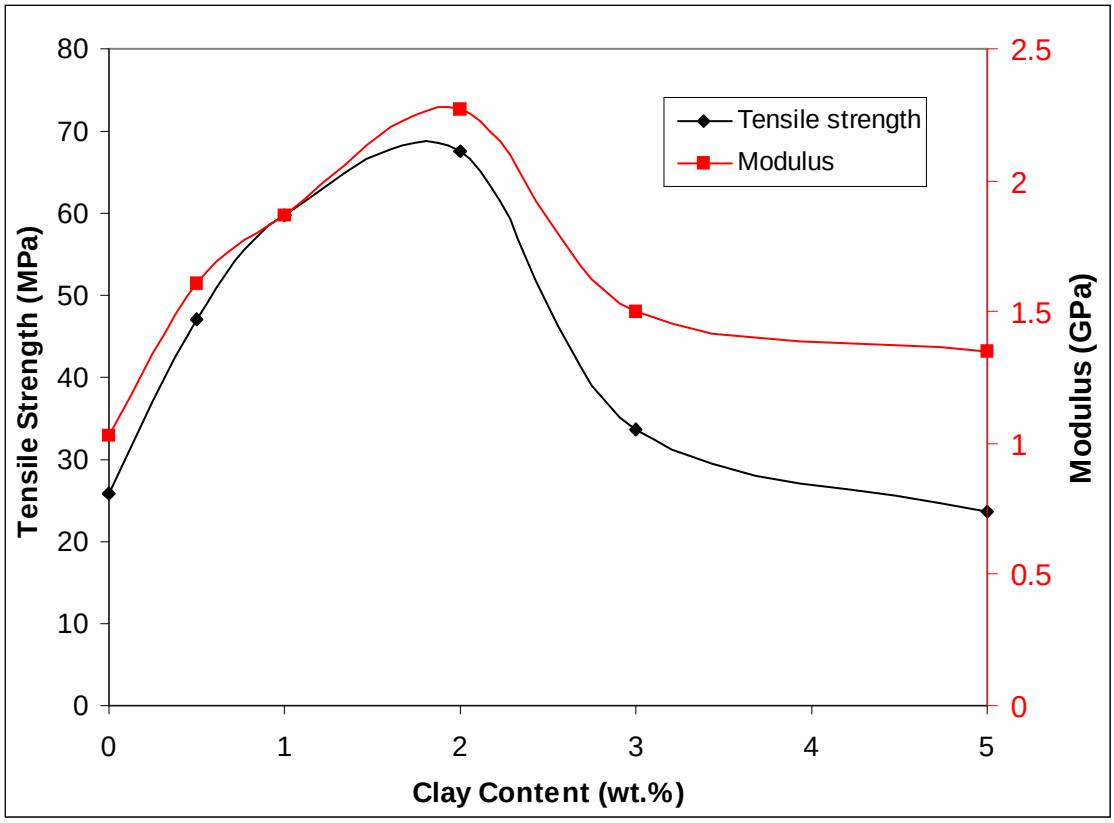

Figure 4.9: Tensile Strength versus Modulus for Polypropylene-Cloisite®15A nanocomposite specimens as a function of clay concentration.

Both the tensile strength and the modulus increase in tandem up to 2 wt. % clay concentration, thereafter significant degradation occurs. The average modulus and tensile strength for 2 wt. % structures is approximately 120 % and 130 % respectively greater than neat polypropylene. These values peak at 2.3 GPa for modulus and 68 MPa for tensile strength as per table 2,

Table 4.1: Tensile Properties of Polypropylene Cloisite®15A Nanocomposites

Specimen	wt. %	Modulus (GPa)		Tensile strength (MPa)	
		Average	Standard Deviation	Average	Standard Deviation
PP-neat	0	1.0	0.021	26	0.502
PP 005	0.5	1.6	0.058	47	0.377
PP01	1	1.9	0.053	60	0.655
PP02	2	2.3	0.044	68	0.803
PP03	3	1.5	0.047	34	0.587
PP05	5	1.4	0.022	22	0.595

A sharp decrease subsequently occurs with 3 wt. % and 5 wt. % specimens dropping to 1.5 GPa and 1.35 GPa respectively. A similar trend for the ultimate tensile strength is shown in figure 3. These findings are consistent to those reported by Kojima *et al.* whose research on polyamide nanocomposites showed stiffness and strength increased by 100 % and 50 % respectively with low nanoclay loadings (less than 4 wt. %) [103, 104, 106]. Ding *et al.* suggests that the increased mechanical properties at low concentration of nanoclays may be due to the uniformly dispersed MMT tactoid and intercalated structures [83]. The organically modified MMT (OMMT) is intercalated by the PP chains and confines the segmental movement of the PP macro-molecules. As a result, the modulus of the PP nanocomposites increases with OMMT loadings. A fraction of intercalated structure decreases with increasing nanoclay content. At higher clay concentrations, aggregation of the nanoclays may occur decreasing the tensile strength and modulus. Failure of 0.5 wt. %, 1 wt. %, and 2 wt. % nanocomposites specimens were very similar to virgin polypropylene specimen. Polypropylene nanocomposite specimens at 3 wt. % and 5 wt. % clay loadings shattered with loud snapping noises at failure which is suggestive of a very brittle failure. R. K. Bharadwaj *et al.* [98] showed that the elastic modulus for polyester nanocomposites significantly decreased for clay concentrations greater than 2 wt. %. The degradation is perhaps linked to the cross-linked bonds decreasing with increasing clay content causing the nanocomposite structures to become more brittle.

4.3.2. Flexural Tests

A minimum of three specimens per category were tested in a three point bend configuration. Figure 4.10 represents the load-deflection data for specimens tested in flexure mode.

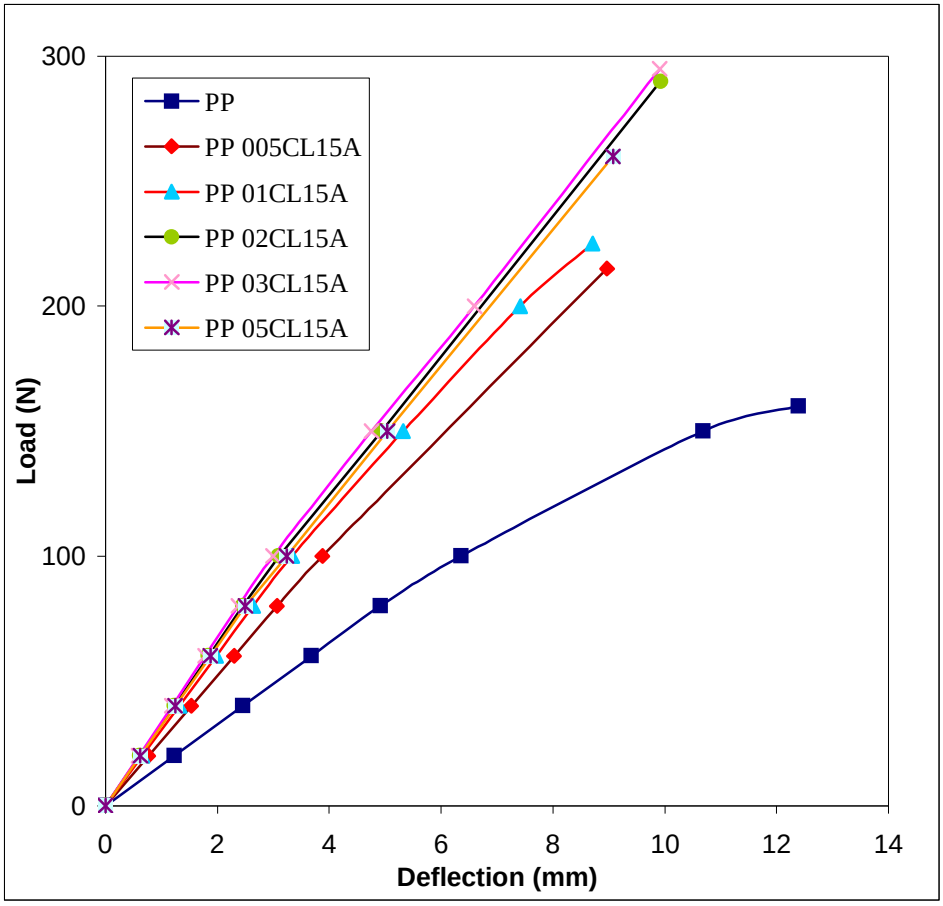

Fig. 4.10: Flexural load versus deflection for virgin and PP nanocomposite specimens.

The flexural properties of the nanophased structures are significantly higher than its neat counterpart. For example, at 0.5 wt % clay loading, the flexural properties increased by 60 %. Further clay loading does not significantly affect the properties and hence specimens with 1 wt. %, 2 wt. %, 3 wt. %, and 5 wt. % clay loadings have similar stiffness. The stiffness gradually increases from 1 wt. % to 3 wt. % with a decrease occurring for 5 wt. % specimens. This is shown in table 4.2.

Table 4.2: Flexural Properties of Polypropylene Cloisite®15A Nanocomposites

Specimen	wt. %	Modulus (GPa)		Flexural strength (MPa)	
		Average	Standard Deviation	Average	Standard Deviation
PP-neat	**0**	**1.5**	**0.028**	**51**	**1.803**
PP 005	**0.5**	**2.3**	**0.057**	**69**	**1.825**
PP01	**1**	**2.7**	**0.058**	**72**	**2.385**
PP02	**2**	**2.9**	**0.028**	**93**	**2.236**
PP03	**3**	**3**	**0.112**	**95**	**1.612**
PP05	**5**	**2.9**	**0.054**	**83**	**2.828**

Flexural strength for nanocomposite specimens correspondingly increased with increasing clay content. PP03CL15A specimens display the highest strength values (94.45 MPa), an increase of approximately 85 %.

4.3.3. Vickers Hardness and Notched Izod Impact Tests

The hardness of the PP nanocomposites gradually increases with increasing clay content similar to the research conducted by Lau *et al*. on epoxy based nanocomposites (105). PP05CL15A specimens displayed the largest hardness numbers averaging at 13.6. The increase in both hardness and impact strength for a nanoclay loading up to 2 wt. % is by the formation of intercalated and exfoliated nanoclay structures shown in the TEM analysis (Figure 4.2, Figure 4.3 and Figure 4.4).

Figure 4.11(a) and 4.11(b) shows an increase in both the impact strength as well as the Vickers hardness number up to 2 wt. % loading.

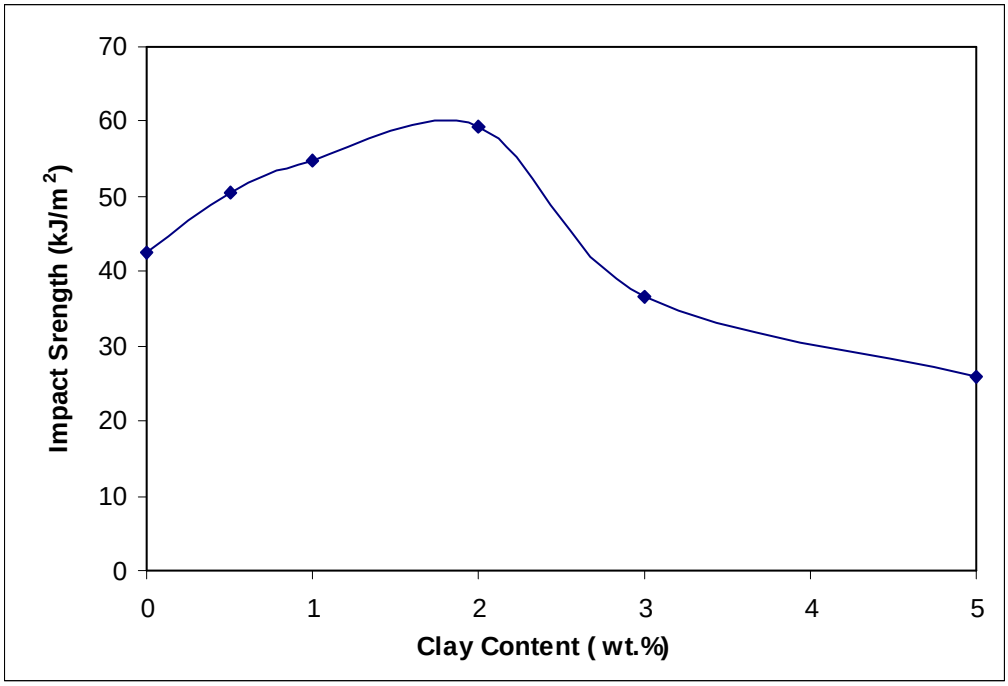

(a)

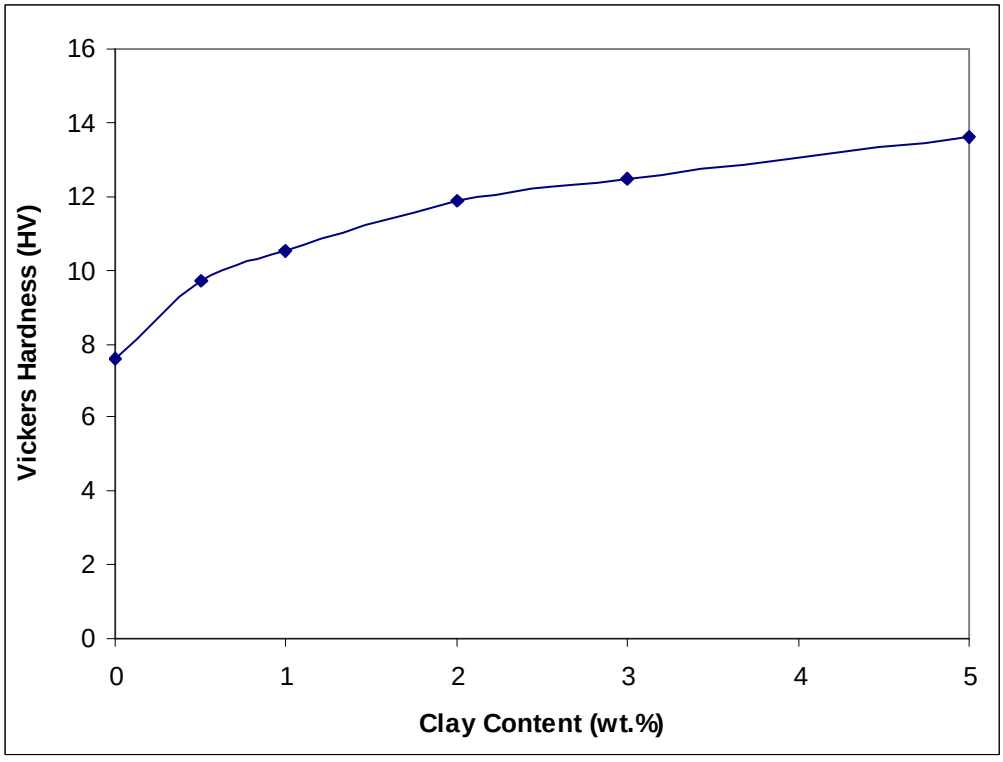

(b)

Fig. 4.11: (a) Impact Strength for virgin and nano-infused polypropylene at various clay loadings, (b) Vickers Hardness for virgin and nano-infused polypropylene at various clay loadings.

Thereafter the impact strength reduces while the hardness number continues to increase. The impact strength decreased due to the formation of agglomerated clay structures at 3 wt. % and 5 wt. % nanoclay loadings which are visible in TEM analysis (figure 4.5 and figure 4.6). Table 4.3 shows the average hardness and impact strengths of the virgin and nano-infused polypropylene specimens.

Table 4.3: Vickers hardness and Impact Properties of virgin PP and nano infused PP

Specimen	wt. %	Vickers Hardness (HV)		Impact strength (kJ/m^2)	
		Average	Standard Deviation	Average	Standard Deviation
PP-neat	0	7.6	0.990	43	1.512
PP 005	0.5	9.7	0.283	51	3.838
PP01	1	10.5	0.721	55	1.370
PP02	2	11.9	0.224	59	5.475
PP03	3	12.5	0.100	37	1.396
PP05	5	13.6	0.640	26	1.565

The exfoliated and intercalated clay platelets dispersed within the polypropylene matrix, at 0.5 wt.%, 2 wt. % and 3 wt. %, acts as crack stoppers causing the crack to follow a tortuous pathway through the matrix and also absorbs impact energy resulting in high impact strengths

4.3.4. Compression testing

The compression stress-strain curves for the virgin polypropylene and polypropylene nanocomposites are shown in Fig. 4.12,

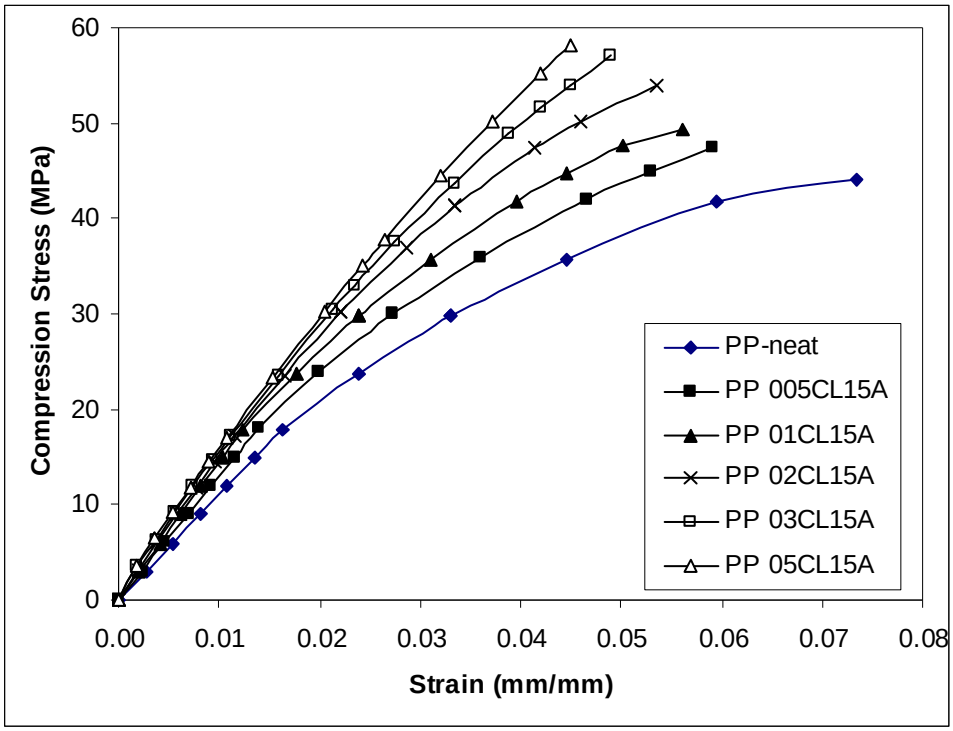

Fig. 4.12: Stress versus strain for Polypropylene-Cloisite®15A nanocomposite specimens loaded in Compression at room temperature (25°C).

Comparison of the slopes of the neat structure and nanocomposite structures in the elastic region indicate an increase in gradient. This increase in slope suggests an increase in the material stiffness with an increase in nanoclay loading up to 5 wt. %. This is suggestive of stiffness increasing with the increasing clay concentration.

Figure 4.13 shows the compression modulus and compressive strength as a function of clay concentration.

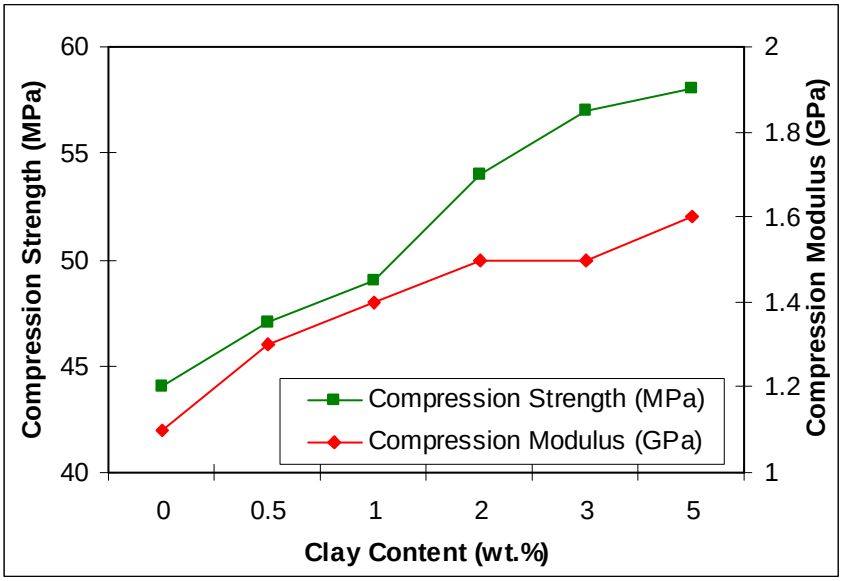

Fig. 4.13: Compression Strength versus Modulus for Polypropylene-Cloisite®15A nanocomposite specimens as a function of clay concentration (wt. %).

The compression strength and modulus for virgin and infused polypropylene is shown in table 4.4.

Table 4.4: Compressive Properties of Polypropylene Cloisite15A Nanocomposites

Specimen	wt. %	Modulus (GPa)		Compressive strength (MPa)	
		Average	Standard Deviation	Average	Standard Deviation
PP-neat	0	1.1	0.064	44	1.208
PP 005	0.5	1.3	0.058	47	1.360
PP01	1	1.4	0.057	49	0.632
PP02	2	1.5	0.014	54	1.217
PP03	3	1.5	0.022	57	1.565
PP05	5	1.6	0.058	58	2.720

The addition of nanoclays has significantly increased to a maximum value of 30 % and 45 % for compression strength and compression modulus, respectively. The stiffness increases due to the formation of intercalated and exfoliated structures at 0.5 wt. % to 2 wt. % in the polypropylene matrix. The uniform distribution of clay tactoids, intercalated and exfoliated nanostructure contributes mainly to the

improvement in the compression properties of polypropylene PP. The compressive strength has progressively increased for 3 wt. % and 5 wt. % polypropylene nanocomposites due to the formation of agglomerated structures at these loadings. The nano clay is intercalated by the PP chains and confines the segmental movement of the PP macro-molecules. As a result, the compressive modulus of the PP nanocomposites increases with clay loadings. This is depicted in the TEM analysis of these structures (figure 4.5 and figure 4.6)

4.4. FRACTURE SURFACE ANALYSIS

Figure 4.14 shows the fractured surface of tensile tested virgin polypropylene. The surface shows a fairly homogenous polymer with minimal high stress zones. The high stress zones, depicted by the lighter lines, were formed by tensile deformation of the matrix.

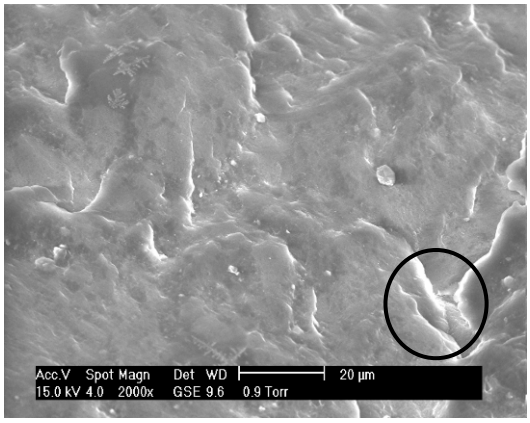

Fig. 4.14: SEM image of the fracture surface of tensile tested virgin PP.

Figure 4.15 shows the fractured surface of polypropylene infused with 0.5 wt. % nanoclays.

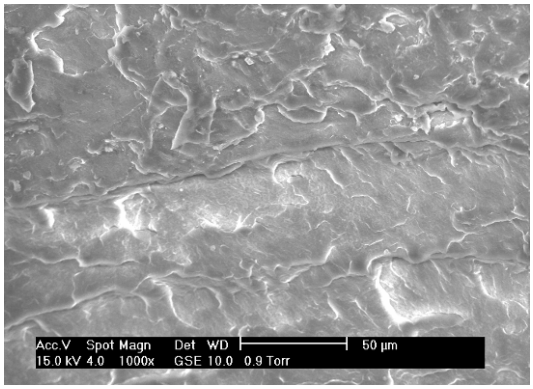

Fig. 4.15: SEM image of the fracture surface of tensile tested
PP infused with 0.5 wt. % nanoclay

There is a distinct change in the fractured surface when compared to virgin PP sample. A network of lighter lines against the grey background and a larger ridge type structure are visible. These structures show several high stress zones which indicate the increased reinforcement of the polymer matrix. These structural phenomena may be linked to the increase in the tensile modulus and tensile strength as shown in table 4.1. The increase in tensile strength may be attributed to the homogenous and fibrillated change in morphology where Chow et al. [106] suggests that good interfacial adhesion results in the enhancement of tensile properties. The 1 wt. % polypropylene nanocomposite structures shown in figure 4.16 has a similar morphology to the 0.5 wt. % structures.

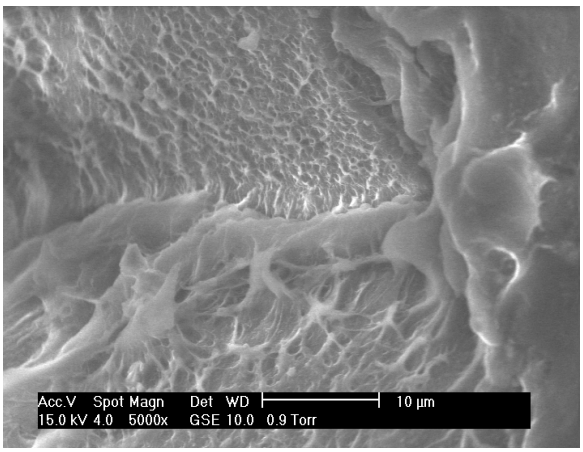

Fig. 4.16: SEM image of the fracture surface of tensile tested
PP infused with 1 wt. % nanoclays.

The fractured surface shows more high stress zones than virgin polypropylene and 0.5 wt. % structures. In line with this, we find that both the stiffness and strength increased to 1.9 GPa and 60 MPa respectively. Figure 4.17 represents the fractured surface of polypropylene infused with 2 wt. % of nanoclays.

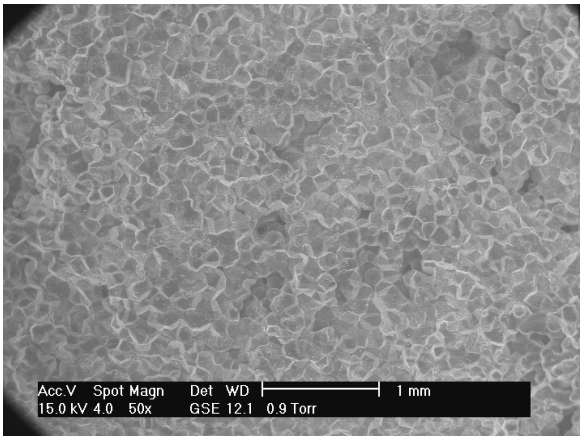

Fig. 4.17: SEM image of the fracture surface of tensile tested
PP infused with 2 wt. % nanoclays.

The structure shown is distinctly different from structures discussed thus far. It is finer and more particulate in nature. This high-density grain boundary shows a strengthened matrix, resulting in increased stiffness and tensile strength as discussed

previously. At this clay loading, maximum enhancement in tensile properties was achieved. Further analysis of the nanocomposite structures at clay loadings greater than 2 wt. % showed a drop in tensile properties. Figure 4.18 represents a magnification of fractured surface of 5 wt. % specimens. Two distinct structures are seen.

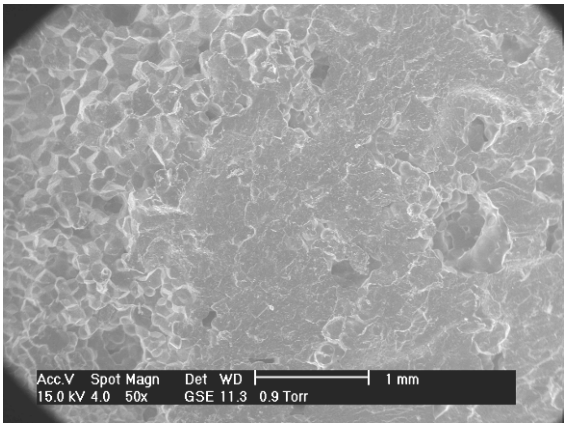

Fig. 4.18: SEM image of the fracture surface of tensile tested
PP infused with 5 wt. % nanoclays;

One is particulate in nature and the other is a large agglomerated structure. The large agglomeration may be a micron sized clay tactoid caused by poor nanoclay dispersion. In order to verify that agglomeration does repeatedly occur at 3 wt. % and 5 wt. % clay loadings, two panels (one 3 wt. % and one 5 wt. %) each measuring 200 × 150 × 6 mm, was manufactured. Five beam type specimens of dimensions 125 × 13 × 6 mm were cut from these panels. The specimens were analysed at two different cross sections along the beam. All of the sections that were scanned showed areas were agglomeration occurred coupled with poor clay dispersion sites. Figure 4.19 shows an image of one of these cross sections, at 5 wt. % clay loading. For closer analysis the fractured surface figure 4.19 image was generated at 20 times magnification, using a light microscope.

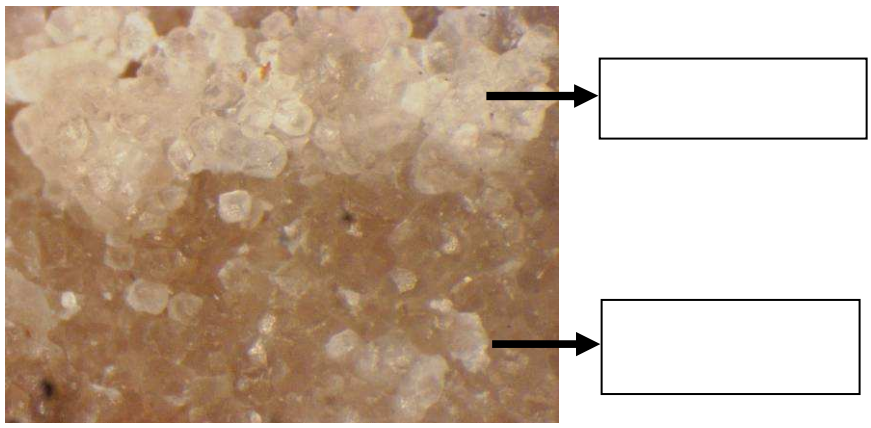

Fig. 4.19: The magnified image of the fractured surface of tensile tested PP infused with 5 wt. % nanoclays.

The fractured surface shows areas where no dispersion occurred and agglomerated clay sites. Preliminary TEM studies indicate that these agglomerated clay tactoids have formed in 5 wt. % structures. These structures impact on the interfacial interactions of the polymer molecules causing poor interfacial adhesion leading to a reduction in tensile properties and embrittlement in the PP nanocomposite structure. These observations are similar to findings reported by Bharadwaj et al., Ding et al., Chow et al., and Gilman et al. [98, 100, 106, 107].

4.5 FRACTURE TOUGHNESS

Fracture toughness was performed on virgin and polypropylene nanocomposites at different weight loadings to analyse the ability of the reinforcing nanoclay structures to resist the crack propagation. The stress intensity factor (K_{IC}) and strain energy release rate (G_{IC}) of neat polypropylene and clay polypropylene nanocomposites is shown in Figure. 4.20.

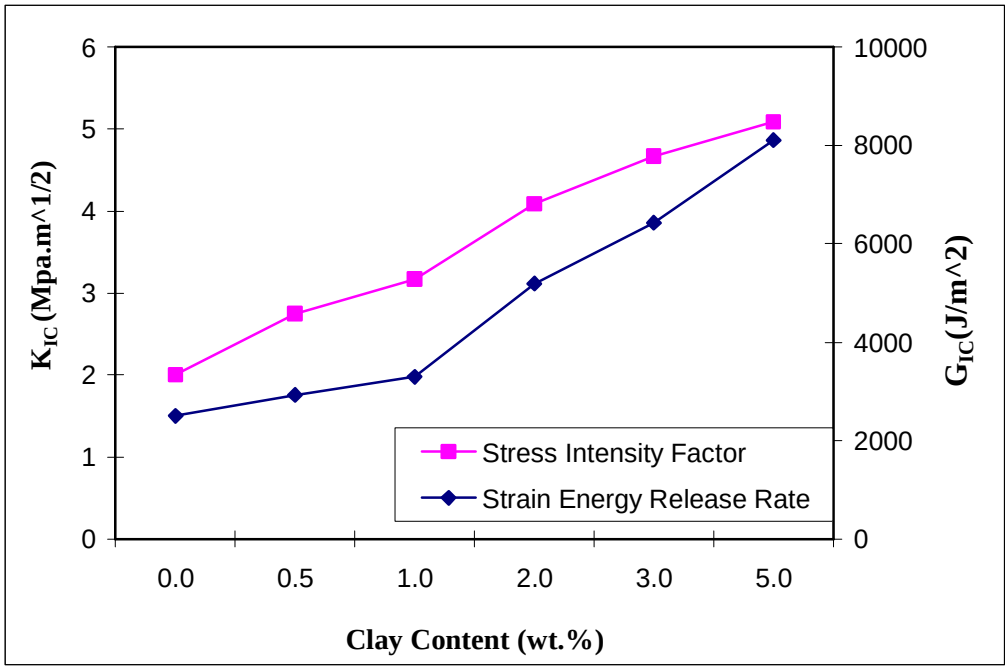

Figure 4.20: Stress Intensity Factor (K_{IC}) and Strain Energy Release Rates (G_{IC}) for virgin PP and PP nanocomposite specimens.

The stress intensity factor (K_{IC}) and strain energy release rate (G_{IC}) of neat polypropylene is 2.00 MPa $m^{1/2}$ and 1765 J/m^2 (Table 4.4).

Table 4.5: Stress Intensity Factor (K_{IC}) and Strain Energy Release Rates (G_{IC}) for nanocomposite specimens.

	Clay Content	**K_{IC}**	**G_{IC}**
specimen	**wt. %**	**Mpa.$m^{1/2}$**	**J/m^2**
PP-neat	0	2.00	2502
PP005CL15A	0.5	2.75	2925
PP01CL15A	1	3.17	3298
PP02CL15A	2	4.09	5191
PP03CL15A	3	4.67	6429
PP05CL15A	5	5.09	8106

The stress intensity factor and strain energy release rate increases on addition of nanoclay. The nanocomposites exhibits a maximum improvement in K_{IC} and G_{IC} for the clay content of 5 wt. %. The improvement in the K_{IC} and G_{IC} values is due to the presence of the intercalated nanoclay structures in the polypropylene nanocomposite

structure. The intercalated nanoclays acts as load bearing agents, and also acts as crack stopping agent. The intercalated dispersion of the clay platelets prevents the easy propagation of the crack by allowing the crack to propagate through torturous pathway resulting in increased fracture resistance and also increases the stress intensity factor and strain energy release rate of the nanoclay infused polypropylene infused specimens.

4.6 DYNAMIC MECHANICAL ANALYSIS

Figure 4.21 shows the storage modulus (E′) at different temperatures for virgin PP and PP with different weight fractions of closite 15A.

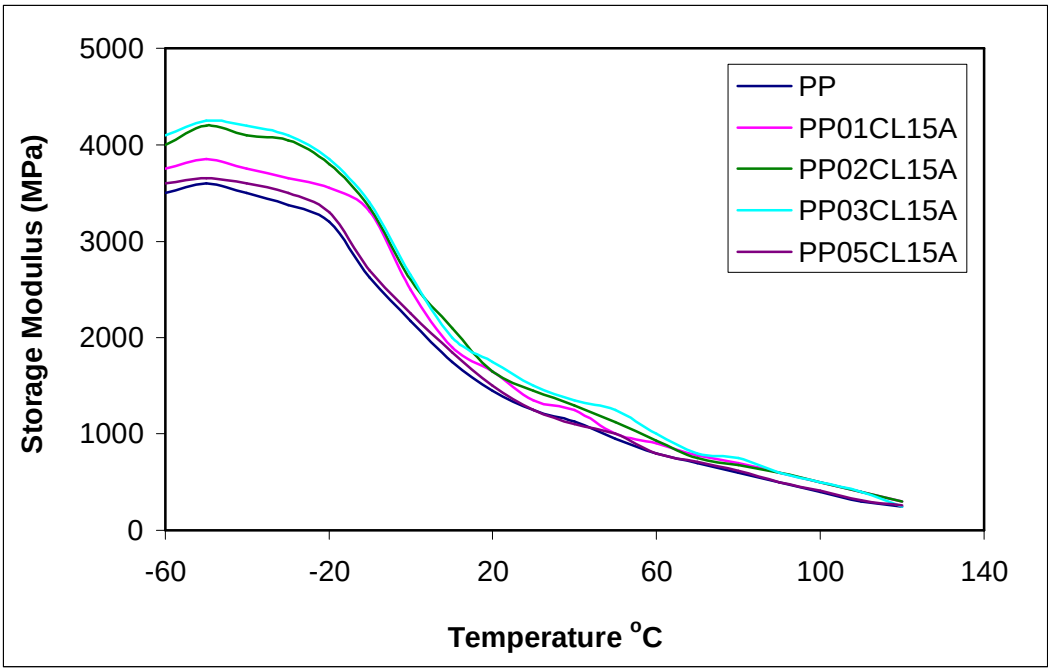

Fig. 4.21: Storage modulus of virgin PP and clay-polypropylene nanocomposites

It was found that the storage modulus of polypropylene increases with addition of closite 15A nanoclays. The storage modulus of neat polypropylene at -60˚C is 3500 MPa. It increases to 3750, 4000, 4100 and 3600 MPa for the clay loadings of 1, 2, 3 and 5 wt. %. We can see an increasing trend in storage modulus on addition of nanoclays up to 3 wt. %. At higher clay content (5 wt. %) the storage modulus

decreases, but it is higher compared to virgin PP. This may be possible that at higher clay content the chance of clay to remain as microtactoids highly contributes in deterioration of the storage modulus. At room temperature, the behavior is almost equivalent. We can also distinguish two apparent changes in storage modulus for both virgin PP and nanocomposite samples. The first change is a sharp drop in storage modulus from -10 to 10˚C and a reduction in rate of drop in storage modulus with temperatures above 40˚ C. the first change between -10 to 10˚ C may be associated with the relaxation of the amorphous phase (α-phase relaxation). In this state, the glassy state of amorphous phase goes through its glass transition temperature and there is a sharp drop in modulus [81]. At higher temperature more than 80˚ C, the transformation rate is less severe. It was evident from DMA curves, that the nanocomposite samples exhibit better storage modulus than virgin PP. Similarly the loss factor curve shows the glass transition temperature (T_g) and softening temperature (T_s) of the virgin PP and the nanocomposite samples corresponding to the peak values of loss factor (Figure 4.22).

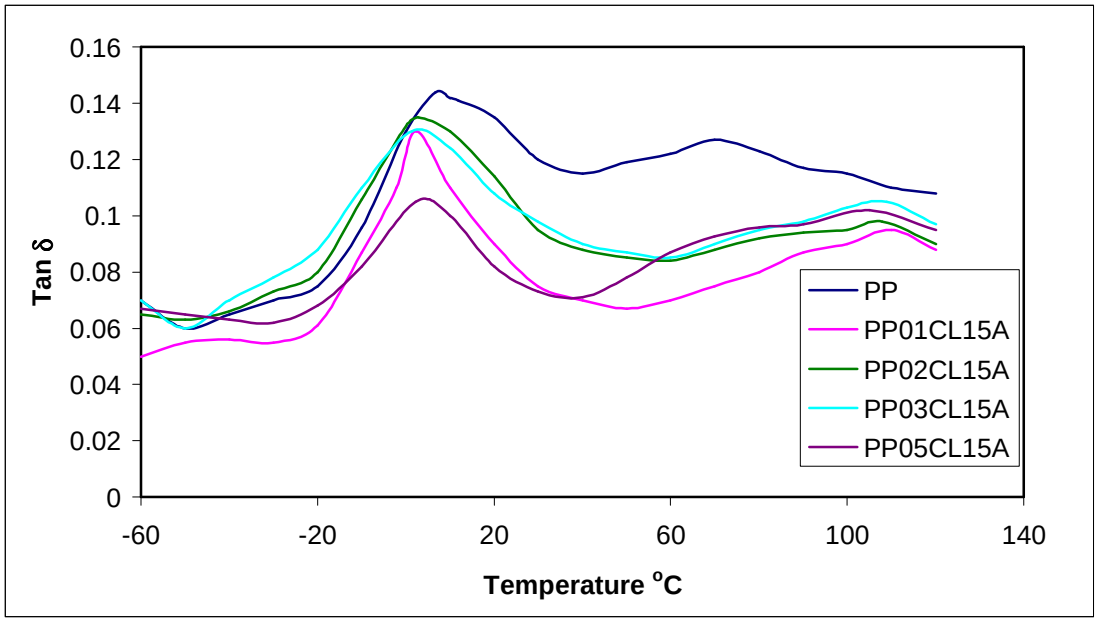

Fig. 4.22: Loss factor curve of virgin PP and clay-polypropylene nanocomposites

The glass transition temperature and softening temperatures are obtained corresponding to the peak values of loss factor. The peak corresponding to low temperature is called glass transition temperature (T_g), second peak at high temperature is corresponding to softening temperature (T_s). It was evident from loss factor curve that, the T_g decreases slightly from 6.76˚C to 2.3, 2.75,1.3 and 2.27˚C for the clay content of 1, 2, 3 and 5 wt.%. However, on the other hand we have noticed a significant increase in softening temperature. The softening temperature increases from 70˚C for PP to 110, 108, 109 and 105˚C for the clay content of 1, 2, 3 and 5 wt.% respectively. The improvement in T_s is the mobility of the amorphous phase in the crystal may be limited by the presence of nanoclays (closite 15A) in the PP matrix.

4.7 TRIBOLOGICAL TESTING

The wear loss of neat PP and nanocomposite samples is shown in Figure 4.23.

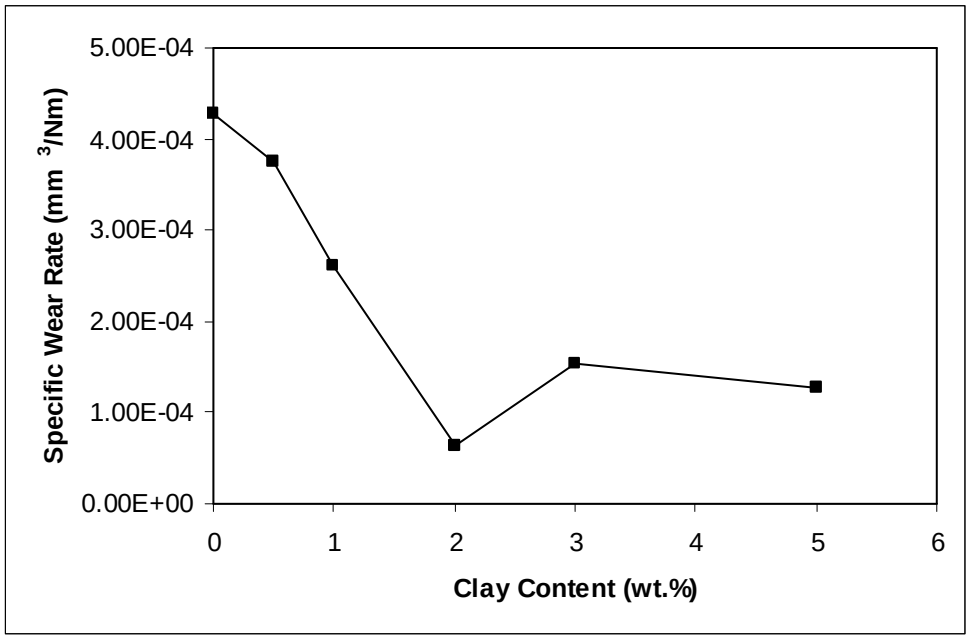

Fig. 4.23: Wear loss of neat PP and nanocomposites

The specific wear rate of neat PP is $4.27e^{-04}$ mm^3/Nm and decreases with the infusion of nanoclays at all the weight loadings.. The specific wear rate of PP with 2wt. % nanoclays decreases to $6.43e^{-05}$ mm^3/Nm while the wear loss of PP with 5 wt. % nanoclays decreases to $1.26e^{-04}$ mm^3/Nm. Nanocomposites with 2 wt.% nanoclay shows a maximum of 85% improvement in wear resistance.. The improvement in wear resistance is mainly attributed to the presence of clay platelets in the PP matrix. These nanosize clay platelets dispersed in the polymer matrix acts as a barrier and also prevent large scale fragmentation of the polymer matrix. The nanoclay platelets dispersed in the polypropylene matrix leads to interfacial strengthening resulting in increased wear resistance [108, 109]. The high interfacial adhesion between the matrix and nanoclay is due to the high specific surface area of the nanoparticles. The nanoparticle having the same size as the segments of the surrounding polymer chains,

the material removal is mild and aids the formation of uniform tenacious transfer film as reported elsewhere [110, 111]. The nanoclay also acts as a reinforcing element, bears the frictional load and reduces wear. Hardness contribution also plays a vital role in wear property improvement [112]. The wear tracks of neat polypropylene and clay polypropylene nanocomposites were analyzed using optical microscopes. The wear track of neat polypropylene is smooth with some deep ploughing marks as shown in Figure 4.24. The mode of material removal is by the ploughing action of the hard asperities of the brass counter disk when the surface of the polypropylene pin slides over the counter face. As neat polypropylene is soft, the asperity in the brass counter face acts as cutting edge and ploughs the material surface and removes the material as wear debris.

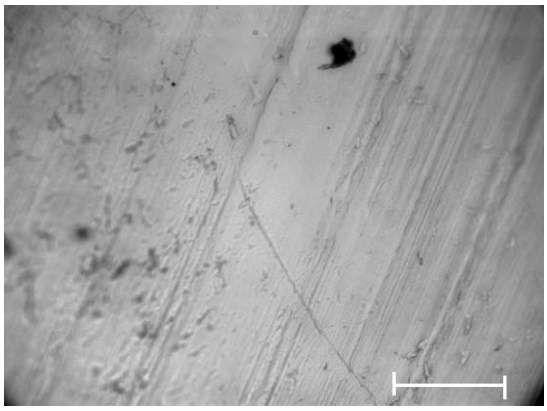

Fig.4.24: Wear surface of neat polypropylene

The optical micrograph shows the wear tracks of nanocomposite samples (Fig. 4.25).

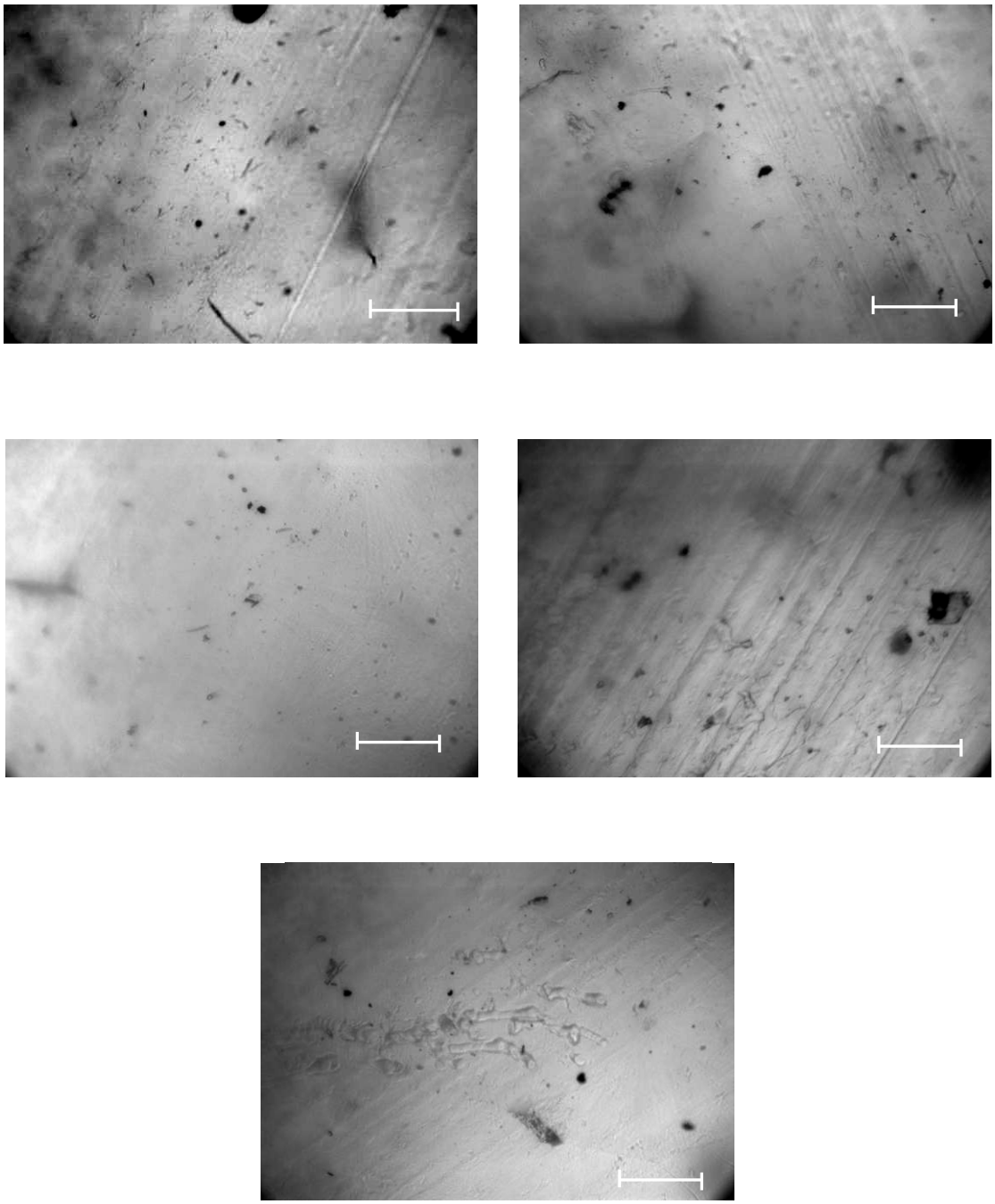

Fig. 4.25: Wear Surfaces of clay polypolypropylene nanocomposites with (a) 0.5 wt.% CL15A, (b) 1 wt.% CL15A, (c) 2 wt.% CL15A, (d) 3 wt.% CL15A, (e) 5 wt.% CL15A.

The wear mechanism is similar in nanocomposite samples. The material is removed from the surface of the nanocomposite test pins by the ploughing and cutting action of asperities. The wear surfaces of the test pins are smooth for the nanocomposites with 0.5, 1 and 2 wt.% clay loadings. The nanocomposite pins with 2. wt.% nanoclay is very fine and it looks that it has got better wear resistant than the neat PP and other nanocomposite samples. It is also evident from the test results that the wear loss is at a minimum for the nanocomposites with 2 wt.% nanoclay. The wear tracks nanocomposites with 3 wt.% and 5 wt.% are comparatively rougher than other nanocomposite samples. Moreover the optical picture for nanocomposites with 5 wt.% nanoclay shows some patches on the surface. The agglomerated clay might have pulled out of the sliding surface and the pulled out regions remains as patch. The nanocomposites with 2 wt.% nanoclay have shown the best wear resistance. The adhesion between the matrix and the intercalated nanoclay platelets is good and leads to the better resistance for nanocomposite samples. The dispersed intercalated nanoclay may also lead to the better adhesion between the films on the counter face [29, 30].

4.8 HALPIN-TSAI MICROMECHANICAL MODEL OF POLYPROPYLENE NANOCOMPOSITES

The tensile and flexural properties of polypropylene are influenced by the manner in which the nanoclays disperse within the polymer matrix. Depending on the nature of the dispersion, increased levels of microstructure reinforcement in the polymer matrix occurs, leading to improvement of properties [102, 113]. However solid state properties are also known to depend on the size and shape of the fillers and their possible orientation with respect to the applied loads. Yi and Sastry indicate

maximum improvement in material properties are achieved with high aspect ratio fibres when a percolation threshold of 4.2 vol. % is reached [101]. They used Monte-Carlo simulations tracking cluster sizes and percolation status in networks of elliptical and circular particles to determine the minimum amount of filler needed to influence properties of a material. A simulation presented in their research shows this threshold percolation volume fraction to be closely related to the particles aspect ratio. In addition to this, Kojima et al. also measured the orientation of MMT clay and polymer crystallites in injection molded specimens of nylon 6-clay nanocomposites [102]. They determined three different regions of orientation as a function of depth, existed in the nanocomposite specimens. Recent studies have demonstrated that the orientation of the clay platelets plays an important role in determining the property enhancement in nanocomposites. Fornes et al. have examined the reinforcement of nylon-6 nanocomposites using composites theories of Halpin–Tsai and Mori–Tanaka [114]. They reported that exfoliated layered silicates offer better reinforcement due to the high modulus, high aspect ratio and its ability to reinforce in two directions. The reinforcing efficiency was found to decrease with increasing number of platelets per stack and with increasing gallery spacing between the platelets. The tensile modulus of intercalated or incompletely exfoliated nanocomposites clay tactoids that are perfectly aligned may thus be calculated from the Halpin–Tsai equation given as;

$$\mathrm{E_A} = \frac{\mathrm{E_{composite}}}{\mathrm{E_{matrix}}} = \frac{1 + 2\mathrm{A}'\eta'\phi'}{1 - \eta'\phi'} \tag{4.1}$$

The modulus of the PP nanocomposite structure may be determined using the ratio, E_A, where A_f' is the aspect ratio of the nanoclay tactoids given by,

$$A'_f = \frac{A_f}{\hat{N}} \left(\frac{1}{1 + \left(1 - 1/\hat{N}\right)\frac{s}{t}} \right) \tag{4.2}$$

A_f, in Eq. (4.2) is the aspect ratio of a single clay platelet (ratio of diameter/thickness), $\hat{N}$ is the number of platelets in an MMT tactoid, s/t is the ratio of distance between clay tactoids to plate thickness and ϕ' corrected volume fraction in intercalated nanocomposite structures. Figure 4.25 shows the comparison between the theoretical modulus predicted from Eq. (4.1) and the experimental measured values from tensile test data.

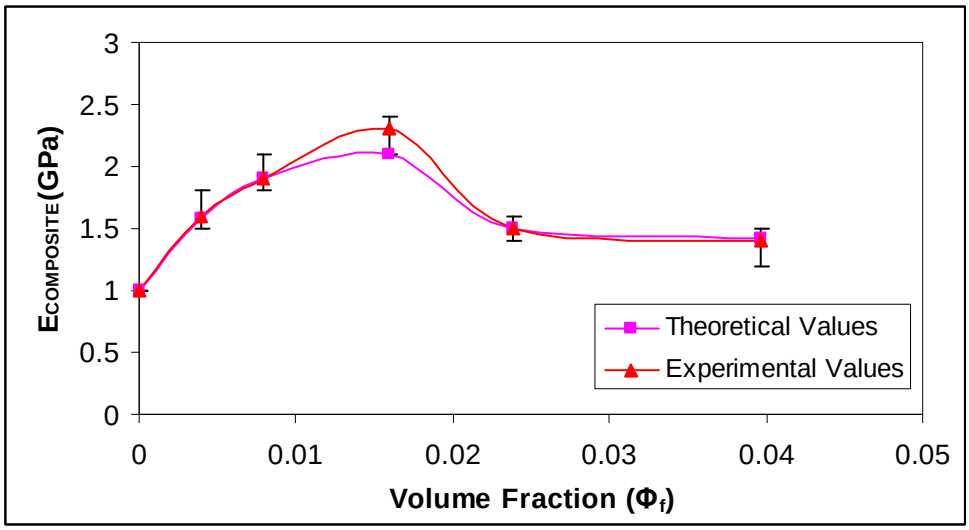

Fig.4.26: Comparison of simulated and experimental moduli of PP nanocomposites as a function of volume fraction.

The input parameters of the model are, modulus of the polypropylene matrix ~ 1 GPa with a density of 0.9 g.cm^{-3}, the modulus of an individual MMT clay platelet ~ 1.72 GPa with a density of 1.66 g.cm^{-3} [86], the average number of platelets in an intercalated MMT clay tactoid which is 4, and the approximate thickness of a clay platelet which is 1 nm. The micromechanical model semi-quantitatively predicts the

modulus of the polypropylene nanocomposites. Initially, at low volume fractions there is fairly good agreement between the theoretical and experimental plots. At volume fractions between 0.5 vol. % and 2.5 vol. %, the model under-estimates the modulus. At volume fractions above 2.5 vol. % there is a satisfactory agreement between the theoretical and experimental results. It is suggested that this micromechanical model provides a fairly reasonable engineering modulus estimate for the polypropylene nanocomposites. However more accurate predictions of the modulus may be obtained by considering the effects of polymer orientation and by solving the full tensorial constitutive equations for nanocomposite structures [65].

CHAPTER 5

SUMMARY AND CONCLUSIONS

5.1. INTRODUCTION

This chapter associates with the conclusions arrived from the processing, characterization, and mechanical testing of thermoplastic polymer nanocomposites. The polymer nanocomposites include various loadings of cloisite 15A nanoclays that are infused into the pristine polypropylene polymer matrix. The conclusions attained from the mechanical properties, tribological properties and morphological analysis of the clay-polypropylene nanocomposites are also discussed.

5.2 CLAY-POLYPROPYLENE NANOCOMPOSITES

The thermoplastic nanocomposites was processed with various weight fractions (0.5, 1, 2, 3, & 5 wt.%) of cloisite 15A nanoclays infused into the virgin polypropylene matrix via melt blending. The nanoclay used for producing nanocomposites is organically treated montmorillonite nanoclay. Tensile modulus increases nearly 2.3 times for polypropylene nanocomposites with 2 wt.% nanoclays. The improvement of the tensile modulus for nanocomposites is due to the exfoliation/intercalation of nanoclay particles in the matrix, which restricts the mobility of polymer chains under loading. The decrease in modulus at higher clay contents may be attributed to the formation of agglomerated clay tactoids. The nanocomposites also show increase in failure strain. Tensile fracture surface analysis of the polypropylene nanocomposites are well corroborated with the mechanical properties. The polypropylene nanocomposites have also displayed better flexural and impact properties. The impact strength of polypropylene is significantly improved with the addition of nanoclay. A

maximum of 8 % improvement in impact strength is noticed for the nanocomposites with 2 wt.% nanoclays. The nano fillers can act as crack stoppers, and form a tortuous pathway for crack propagation, resulting in higher impact energy. The presence of exfoliated and intercalated clay platelets in the polypropylene nanocomposites effectively restricts indentation thereby possessing excellent hardness. The hardness has increased to a maximum of 80 % for 5wt. % loadings. The wear loss decreases on the addition of nanoclays. The wear loss is reduced significantly especially for the clay content of 2 wt.% nano-size clay platelets dispersed in the polymer matrix and acts as a barrier preventing large scale fragmentation of the polymer matrix. The nanoclay platelets dispersed in the polypropylene matrix leads to interfacial strengthening resulting in increased wear resistance [24, 25]. The improvement in wear resistance is mainly attributed to the presence of clay platelets in the PP matrix.

5.3 CONCLUSIONS

1. In the XRD analysis of the pristine polypropylene and polypropylene nanocomposites, the disappearance of the peak in the PP nanocomposites indicates the separation of clay layers and the formation of intercalated or exfoliated structures. This is confirmed in the transmission electron microscopic studies.
2. TEM images at 0.5 wt. %, 1 wt. %, and 2 wt. % clay loadings show evidence of intercalated and exfoliated structures. These structures may be responsible for the increase in properties at low weight loadings.
3. TEM and SEM images of 5 wt. % structures show areas of poor clay infusion and multiple agglomerations sites. The agglomerated clay tactoids are visible

on the fractured surface of 5 wt. % specimens may be responsible for the degradation in properties.

4. The tensile strength and tensile modulus increases by 160 % and 45 % respectively, at a threshold of 2 wt. % nanoclay loadings, while flexural strength and flexural modulus increases by 85 % and 100 % respectively, at a threshold of 3 wt. % nanoclay loadings. The tensile and flexural properties then degrade at higher nanoclay weight loadings.
5. The compression strength of PP nanocomposites shows an increase in material stiffness with an increase in nanoclay loading up to 5 wt. %. This is suggestive of the stiffness increasing with increasing clay concentration.
6. SEM studies of the tensile fractured surfaces at low clay loadings shows that the morphology changes to homogenous and fibrillated. This indicates there is good interfacial adhesion between the nanoclays and polymer which may be responsible for the improvement in tensile strength.
7. Increased fracture resistance, increased stress intensity factors (K_{IC}) and strain energy release rates (G_{IC}), by approximately 150 % and 120 %, respectively at 5 wt. % loadings are indicated in fracture toughness tests. This is due to the formation of dispersed intercalated clay platelets in the PP nanocomposites that stops the easy propagation of cracks by causing the crack to propagate through a torturous pathway.
8. It was found that the storage modulus of PP increases with addition of closite 15A nanoclays up to 5 wt. % loadings. An increasing trend in the storage modulus, by 17 %, is shown on addition of nanoclays up to 3 wt. %. There is a minimal decrease for 5 wt. % loadings, however, this is more improved than the virgin polypropylene storage modulus.

9. Loss factor curves show an improvement in the softening temperature for PP nanocomposites indicating that the mobility of the amorphous phase in the crystal may be limited by the presence of nanoclays in the PP matrix**.**
10. Polypropylene infused with 2 wt. % of nanoclays has shown significant reduction in wear rate. The improvement in wear resistance is mainly attributed to the presence of clay platelets in the PP matrix. The nanosize clay platelets, dispersed in the polymer matrix, act as a barrier and also prevent large scale fragmentation of the polymer matrix.

REFERENCES

1. **Richardson, T.,** (1987), "Composites A Design Guide", Industrial Press Inc, New York.

2. **Anderson, J.C., Leaver K.D., Rawlings R.D. and Alexander J.M.** (1990), Material Science and Engineering, Chapman and Hall India, Madras, India. 1969.

3. **Deborah, D.L.C.,** (2002), Composite Materials: Science and Applications Functional Materials for Modern Technologies, Springer, London.

4. **Ajayan, P.M., Schadler L.S. and Braun P.V.,** (2003), Nanocomposite Science and Technology., Wiley-VCH GmbH & Co. KgaA,

5. **Pinnavaia, T.J. and Beall G.W.,** (2002), Polymer-Clay Nanocomposites, John Wiley & Sons, Ltd, New York,

6. **Hay, J.N.** (2000), "A Review of Nanocomposites 2000", Retrieved August 10, 2006, from http://www.azom.com/details.asp?ArticleID=921

7. **Nanocompositech.com, "**Clay polymer nanocomposites: Brief outline", Retreived August 12, 2006 from http://www.nanocompositech.com/review-nanocomposite.htm.

8. **Demetrakakes, P.,** (2002), "Nanocomposites raise barriers, but also face them: Clay-based additives increase the barrier qualities of plastics, but obstacles to commercialization must be overcome", Nanocomposite Materials, Retrieved February 16, 2004, from

   http://www.findarticles.com/p/articles/mi_m0UQX/is_12_66/ai_96123509

9. **Leaversuch, R.,** (2001), "Nanocomposites broaden roles in automotive, barrier packaging", Plastics Technology. Retrieved February 16, 2004, from EBSCOhost database.

10. **Biswas, M. and Sinha, R. S.,** (2001), "Recent progress in synthesis and evaluation of polymer–montmorillonite nanocomposites" Advances in Polymer Science, **155**, pp. 167–221.

11. **Giannelis, E. P.,** (1996), "Polymer layered silicate nanocomposites", Advanced Materials, **8**, pp. 29–35.

12. **Giannelis, E. P., Krishnamoorti, R. and Manias, E.,** (1999), "Polymer-silicate nanocomposites: model systems for confined polymers and polymer brushes" Advances in Polymer Science, **138**, pp. 107–147.

13. **Lebaron, P.C., Wang, Z. and Pinnavaia T. J.,** (1999), "Polymer-layered silicate nanocomposites: an overview", Applied Clay Science, **15**, pp. 11–29.

14. **Vaia, R.A., Price G., Ruth P.N., Nguyen H.T. and Lichtenhan J.,** (1999), "Polymer/layered silicate nanocomposites as high performance ablative materials", Applied Clay Science. **15**, 67–92.

15. **Giannelis, E.P.,** (1998), "Polymer-layered silicate nanocomposites: synthesis, properties and applications", Applied Organomettalic Chemistry, **12**, 675–680.

16. **Xu, R., Manias E., Snyder A. J., and Runt J.,** (2001), **"**New biomedical poly(urethane urea)-layered silicate nanocomposites", Macromolecules, **34**, pp. 337–339.

17. **Bharadwaj, R. K.,** (2001), "Modeling the barrier properties of polymer layered silicate nanocomposites", Macromolecules, **34,** pp. 1989–1992.

18. **Messersmith, P. B., and Giannelis, E. P.,** (1995), "Synthesis and barrier properties of poly(1-caprolactone)-layered silicate nanocomposites", Journal of Polymer Science, Part A: Polymer Chemistry, **33,** pp**.** 1047–1057.

19. **Yano, K., Usuki A., Okada A., Kurauchi, T., and Kamigaito, O.,** (1993), "Synthesis and properties of polyimide–clay hybrid", Journal of Polymer Science, Part A: Polym Chem, **31**, pp. 2493–2498.

20. **Kojima, Y., Usuki A., Kawasumi M., Fukushima Y., Okada A., Kurauchi T. and Kamigaito O.,** (1993), "Synthesis of nylon 6–clay hybrid", Journal of Materials Research, 8**,** pp. 1179–1184.

21. **Gilman, J. W., Kashiwagi, T. and. Lichtenhan, J. D,** (1997), "Flammability studies of polymer-layered silicate nanocomposites", SAMPE Journal, **33**, pp. 40–45.

22. **Gilman, J. W,** (1999), "Flammability and thermal stability studies of polymer-layered silicate (clay) nanocomposites", Applied Clay Science, **15**, pp. 31–49.

23. **Gilman, J. W., Jackson C. L., Morgan A. B., Harris J. R, Manias E., Giannelis E. P. , Wuthenow M., Hilton D. and Phillips S. H.,** (2000), "Flammability properties of polymer-layered silicate nanocomposites. Propylene and polystyrene nanocomposites" Chemistry of Materials, **12**, pp. 1866–1873.

24. **Dabrowski, F., Bras M. L., Bourbigot S., Gilman J. W. and Kashiwagi T., (1999),"**PA-6 montmorillonite nanocomposite in intumescent fire retarded EVA", Proceedings of Eurofillers 99, France, September, 6-9.

25. **Bourbigot, S., Lebras M., Dabrowski F., Gilman J. W. and Kashiwagi T.,** (2000), "PA-6 clay nanocomposite hybrid as char forming agent in intumescent formulations", Fire and Materials, **24**, pp. 201–208.

26. **Sinha, R. S., Yamada K., Okamoto M. and Ueda K.,** (2002), "New polylactide/layered silicate nanocomposite: a novel biodegradable material", Nano Letters, **2**, pp. 1093–1096.

27. **Vaia, R.A. and Giannelis E.P.,** (1997a), "Polymer melts intercalation in organically-modified layered silicates: model predictions and experiment", Macromolecules, **30**, pp. 8000–8009.

28. **Vaia, R.A. and E.P. Giannelis,** (1997b), 'Lattice of polymer melt intercalation in organically-modified layered silicates", Macromolecules, **30**, pp. 7990–7999.

29. **Vaia, R.A,, Kramer E.J. and Giannelis E.P.,** (1995), "Kinetics of polymer melts intercalation", Macromolecules, **28**, pp. 8080–8085.

30. **Lee, J.Y., Baljon A.R.C., Loring R.F. and Panagiopoulos A.Z.,** (1998), "Simulation of polymer melt intercalation in layered nanocomposites", Journal of Chemical Physics, **109,** pp. 10321–10330.

31. **Balazs A.C., Singh C. and Zhulina E.,** (1998), "Modeling the interactions between the polymers and clay surfaces through self-consistent field theory" Macromolecules, **31**, pp. 8370-8381.

32. **Hackett, E., Manias E. and Giannelis E.P.,** (1998), "Molecular dynamics simulations of organically modified layered silicates" Journal of Chemical Physics, **108,** pp. 7410–7415.

33. **Hackett, E., Manias E. and Giannelis E.P.,** (2000), **"**Computer simulation studies of PEO/layered silicate nanocomposites", Chemistry of Materials, **12**, pp. 2161–2167.

34. **Anastasiadis, S.H., Karatasos K., Vlachos G., Manias E. and Giannelis E.P.,** (2000), "Nanoscopic-confinement effects on local dynamics" Physical Review Letter; **84**, pp. 915–918.

35. **Blumstein, A.**, (1965), "Polymerization of adsorbed monolayers: II Thermal degradation of the inserted polymers", Journal of Polymer Science Part A: Polymer Chemistry, **3**, pp. 2665–2673.

36. **Okada, A., Kawasumi M., Usuki A., Kojima Y., Kurauchi T. and Kamigaito O.,** (1990), "Synthesis and properties of nylon-6/clay hybrids. Polymer based molecular composites", MRS Symposium Proceedings, **171**, pp. 45–50.

37. **Vaia, R.A., Ishii H. and Giannelis E.P.,** (1993), "Synthesis and properties of two-dimensional nanostructures by direct intercalation of polymer melts in layered silicates", Chemistry of Materials, **5**, pp. 1694–1696.

38. **Sinha, R.S, Okamoto K. and Okamoto M.,** (2003), "Structure–property relationship in biodegradable poly(butylenes succinate)/layered silicate nanocomposites" Macromolecules, **36**, pp. 2355–2367.

39. **Brindly, S.W. and Brown G., "**Crystal structure of clay minerals and their X-ray diffraction", London: Mineralogical Society, 1980.

40. **Aranda, P. and Ruiz-Hitzky E.,** (1992), "Poly(ethylene oxide)-silicate intercalation materials", Chemistry of Materials, 4, pp. 1395–1403.

41. **Greenland, D.J.,** (1963), "Adsorption of poly(vinyl alcohols) by montmorillonite", Journal of Colloid and Interface Science, **18**, pp. 647–664.

42. **Lagaly, G.,** (1986), "Interaction of alkylamines with different types of layered compounds", Solid State Ionics, **22**, pp. 43–51.

43. **Usuki, A., Kawasumi M., Kojima Y., Okada A., Kurauchi T. and Kamigaito O.,** (1993), "Synthesis of nylon-6-clay hybrid", Journal of Materials Research, **8**, pp. 1174-1178.

44. **Lan, T., Kaviratna P.D. and Pinnavaia T. J.,** (1995), "Mechanism of clay tactoid exfoliation in epoxy-clay nanocomposites", Chemistry of Materials, **7**, pp. 2144-2150.

45. **Maharaphan, R., Lilayuthalert W., Sirivat A. and Schwank J.W.,** (2001), "Preparation, structure, properties and thermal behavior of rigid-rod polyimide / montmorillonite nanocomposites". Composites Science and Technology, **61**, pp. 1253–1264.

46. **Kornmann, X. and Berglund L.A.,** (1998), "Nanocomposites Based on Montmorillonite and Un-saturated polyester", Polymer Engineering and Science, **38**, pp. 1351-1358.

47. **Krishnamoorti, R.K., Vaia R.A. and Giannelis E.P.,** (1996), "Structure and dynamics of polymer-layered silicate nanocomposites", Chemistry of Materials, **8**, pp. 1728–1734.

48. **Vaia, R.A., Teukolsky, R.K. and Giannelis E.P.,** (1994), "Interlayer structure and molecular environment of alkylammonium layered silicates", Chemistry of Materials, **6**, pp. 1017–1022.

49. **Sinha, R.S, Okamoto, K. and Okamoto M.,** (2003), "Structure–property relationship in biodegradable poly(butylenes succinate)/layered silicate nanocomposites" Macromolecules, **36**, pp. 2355–2367.

50. **Vaia, R.A, Jant K.D., Kramer E.J. and Giannelis E.P.,** (1996), "Microstructural evaluation of melt-intercalated polymer-organically modified layered silicate nanocomposites", Chemistry of Materials, **8**, pp. 2628–2635.

51. **Morgan, A.B. and Gilman J.W.,** (2003), "Characterization of poly-layered silicate (clay) nanocomposites by transmission electron microscopy and X-ray diffraction: a comparative study", Journal of Applied Polymer Science. **87**, pp. 1329–1338.

52. **Aranda, P. and Ruiz-Hitzky E.**, (1992), "Poly(ethylene oxide)-silicate intercalation materials", Chemistry of Materials, **4**, pp. 1395–1403.

53. **Francis, C.W.,** (1973), "Adsorption of polyvinylpyrrolidone on reference clay minerals", Soil Science, **115**, pp. 40–54.

54. **Zhao, X., Urano K. and Ogasawara S.,** (1989), "Adsorption of poly(ethylene vinyl alcohol) from aqueous solution on montmorillonite clays" Colloid and Polymer Science, **267,** pp. 899–906

55. **Jimenez, G., Ogata N., Kawai H. and Ogihara T.,** (1997), "Structure and thermal/mechanical properties of poly(1-caprolactone)–clay blend", Journal of Applied Polymer Science, **64**, pp. 2211–2220.

56. **Ogata, N, Jimenez G., Kawai H. and Ogihara T.,** (1997), "Structure and thermal/mechanical properties of poly(L-lactide)–clay blend", Journal of Polymer Science Part B: Polymer Physics, **35**, pp. 389–396.

57. **Jeon, H.G., Jung H.T., Lee S.W. and Hudson S.D.,** (1998), "Morphology of polymer silicate nanocomposites. High density polyethylene and a nitrile copolymer", Polymer Bulletin, **41**, pp. 107–113.

58. **Kawasumi, M., Hasegawa N., Usuki A. and Okada A.,** (1998), "Nematic liquid crystal/clay mineral composites", Material Science and Engineering C, **6**, pp. 135–143.

59. **Wang, Z. and Pinnavaia T.J.,** (1998a), "Nanolayer reinforcement of elastomeric polyurethane", Chemistry of Materials, **10**, pp. 3769-3771.

60. **Ke, Y., Long C. and Qi Z.,** (1999), "Crystallization, properties, and crystal and nanoscale morphology of PET clay nanocomposites", Journal of Applied Polymer Science, **71**, pp. 1139-1146.

61. **Lan, T. and Pinnavaia T. J.,** (1994), "Clay-reinforced epoxy nanocomposites", Chemistry of Materials, **6**, pp. 2216-2219.

62. **Shi, H., Lan T. and Pinnavaia T. J.,** (1996), "Interfacial effects on the reinforcement properties of polymer organoclay nanocomposites", Chemistry of Materials, **8**, pp. 1584-1587.

63. **Usuki, A., Koiwai A., Kojima Y., Kawasumi M., Okada A., Kurauchi T., and Kamigaito O.,** (1995), "Interaction of nylon 6-clay surface and mechanical

properties of nylon 6-clay hybrid", Journal of Applied Polymer Science, **55**, pp. 119-123.

64. **Kojima Y, Usuki A, Kawasumi M, Okada A, Fukushima Y, Kurauchi T, and Kamigaito O.** (1993b), "Mechanical properties of nylon 6–clay hybrid", Journal Materials Research, **8**, pp. 1185–1189.

65. **Fornes, T.D. and Paul D.R.,** (2003), "Modelling properties of nylon6/clay nanocomposites using composites theories", Polymer, **44,** pp. 4993-5013.

66. **Yano, K, Usuki A., Okada A., Kurauchi T. and Kamigaito O.,** (1991), "Synthesis and properties of polyimide–clay hybrid", Polymeric Preprints, **32,** pp. 65–67.

67. **Yano, K, Usuki, A., Okada, T. Kurauchi and O. Kamigaito,** (1993), "Synthesis and properties of polyimide–clay hybrid", Journal of Polymer Science, Part A: Polym Chem, **31**, pp. 2493–2498.

68. **Yano K, Usuki A. and Okada A.,** (1997), "Synthesis and properties of polyimide–clay hybrid films", Journal of Polymer Science, Part A: Polymer Chemistry, **35**, pp. 2289–2294.

69. **Honeywell International, Inc,** (2004), Honeywell Capran® Films: Flexible packaging. Retrieved February 16, 2004, from http://www.honeywell.com/sites/sm/capran/flexible_packaging.htm

70. **Leaversuch, R.,** 2003, "Barrier PET bottles", Plastics Technology. Retrieved February 16, from http://www.plasticstechnology.com/articles/2003 03fa2.html

71. **Fujiwara, S. and Sakamot T.**, (1976), "Flammability properties of Nylon-6/mica nanocomposites", Kokai patent application, no. SHO51, 1976-109998.

72. **Nam, P.H., Maiti P., Okamaoto M.and Kotaka T.,** (2001), "Foam processing and cellular structure of polypropylene/clay nanocomposites", Proceedings of Nanocomposites, ECM Publication, Chicago, Illinois, USA, June, 2001.

73. **Sinha, R.S., Yamada K., Okamoto M. and Ueda K.,** (2003b), "New polylactide/layered silicate nanocomposites. 2. Concurrent improvements of material properties, biodegradability and melt rheology", Polymer, **44**, pp. 857–866.

74. **Wang, Z., Lan T., and Pinnavaia T. J.,** (1996), "Hybrid organic-inorganic nanocomposites formed from an epoxy polymer and a layered silicic acid (Magadite)", Chemistry of Materials, **8**, pp. 2200-2204.

75. **Wang, Z. and Pinnavaia T.J.,** (1998a), "Nanolayer reinforcement of elastomeric polyurethane", Chemistry of Materials, **10**, pp. 3769-3771.

76. **Mirabella M. Francis, Jr**., (2004), "Polypropylene and TPO Nanocomposites", Dekker Encyclopedia of Nanoscience and Nanotechnology, **5,** pp. 3015-3038

77. **Ma, J.S., Qi, Z.N., and Hu, Y.L.,** 2001, "Synthesis and characterization of polypropylene/clay nanocomposites", Journal of Applied Polymer Science, 82, pp. 3611-3617

78. **Manias, E.,** 2001, "A direct-blending approach for polypropylene/clay nanocomposites enhances properties", Materials Research Society Bulletin, **26**, pp. 862 - 863

79. **Pinnavaia, T.J. (Ed.),** 2000, "Polymer–Clay Nanocomposite", Wiley, London

80. **Kato, M., Y., Usiki, A., and Okada, A**., 1997, "Synthesis of Polypropylene Oligomer-Clay Intercalation Compounds", Journal of Applied Polymer Science, **66**, pp. 1781-1785

81. **Lei, S**, **Hoa, S**. **V.G.**, **Ton-That M.-T**, 2006, "Effect of clay types on the processing and properties of polypropylene nanocomposites", Composites Science and Technology, **66,** pp. 1274-1279

82. **Bertini, F**., **Canetti, M.**, **Audisio, G.**, **Costa, G**., **and Falqui L**., 2005, "Characterization and thermal degradation of polypropylene-montmorillonite nanocomposites", Polymer Degradation and Stability, **91**, pp. 600-605

83. **Ding, C**., **Jia, D., Hui, H., Guo, B., and Hong, H**., 2004, "How Organo-Montmorillonite Truly Affects The Structure And Properties Of Polypropylene", Polymer Testing, **20**, pp. 1-7.

84. **Peter, R**., **Hansjörg, N., Stefan, K., Rainer, B., and Ralf, T. R.**, 2001, "Poly(propylene)/organoclay nanocomposite formation: Influence of compatibilizer functionality and organoclay modification", Macromolecular Materials and Engineering, **1**, pp. 8-17

85. **Qin, H**., **Zhang, S., Zhao, C., Feng, M., Yang, M., Shu, Z., and Yang, S.**, 2004, "Thermal stability and flammability of polypropylene/montmorillonite composites" Polymer Degradation and Stability, **85**, pp. 807-813

86. **Galgali, G**., **Agarwal, S., and Lele, A**., 2004, "Effect of clay orientation on the tensile modulus of polypropylene-nanoclay composites", Polymer Journal, **45**, pp. 6059 – 6069

87. **Chang, L, Zhang Z., Breidt C. and Friedrich K.,** (2005), "Tribological properties of epoxy nanocomposites I. Enhancement of the wear resistance by nano-TiO2 particles", Wear, **258**, pp. 141 – 148

88. **Zhang, Z., Haupert F. and Friedrich, K,** (2003), "Enhancement on wear resistance of polymer composites by nano-fillers", German Patent Application No. 10329228.4.

89. **Zhang, Z., Breidt, C., Chang L., Haupert F. and Friedrich K.,** (2004), "Enhancement on wear resistance of epoxy: short carbon fibre, Graphite, PTFE and Nano-TiO2", Composites Part A: Applied Science and Manufacturing, **35**, pp. 1385–1392

90. **Wang, Q.H, Xue Q.J. and Shen W.,** (1997), "The friction and wear properties of nanometre SiO_2 filled Polyetheretherketone", Tribology international, **30,** pp. 193-197

91. **Wang, Q.H., Xue Q., Shen W. and Zhang J.,** (1998), "The friction and wear properties of nanometer ZrO_2-filled polyetheretherketone", Journal of Applied Polymer Science, **69,** pp. 135-141.

92. **Wang, Q.H., Xu J.F., Shen W.C. and Xue Q.J.**, (1997), "The effect of nanometer SiC filler on the tribological behavior of PEEK", Wear, **209**, pp. 316–321.

93. **Wang, Q.H., Xue Q.J., Liu W.M. and Chen J.M.**, (2001), "Tribological characteristics of nanometer Si_3N_4 filled poly(ether ether ketone) under distilled water lubrication", Journal of Applied Polymer Science, **79,** pp. 1394-1400.

94. **Sawyer, W.G., Kevin D., Berg F., Bhimaraj P. and Schadler L.S.,** (2003), "A study on the friction and wear behavior of PTFE filled with alumina nanoparticles", Wear, **254**, pp. 573–580.

95. **Shi, G., Zhang M.Q., Rong M.Z., Wetzel B. and Friedrich K.,** (2004), "Sliding wear behavior of epoxy containing nano-Al_2O_3 particles with different pretreatments", Wear, **256**, pp. 1072–1081

96. **ASTM D 3039 / D 3039M -93**, (2004), "Standard Test Method for tensile properties of polymer matrix composite materials", ASTM Book of Standards, **08**, Plastics (I): D256 - D2343

97. **ASTM D 256-02e1**, (2004), "Standard Test Methods for Determining the Izod Pendulum Impact Resistance of Plastics, ASTM Book of Standards, **08.01**, Plastics (I): D256 - D2343.

98. **Bharadwaj**, **R.K**., (2002), "Structure-Property Relationships in Cross-Linked Polyester-Clay Nanocomposites", Polymer Journal, **43**, pp. 3699-3705.

99. **Utracki, L**. **A.**, **and Kamal, M.R.**, (2002), "Clay-Containing Polymeric Nanocomposites", The Arabian Journal for Science and Engineering, **27**, pp. 43-67.

100. **Ding, C**., **Jia**, **D., Hui, H., Guo, B., and Hong, H.**, (2004), "How Organo-Montmorillonite Truly Affects The Structure And Properties Of Polypropylene", Polymer Testing, **20**, pp. 1-7.

101. **Sastry, A. M., and Yi, Y. B.**, (2002), "Analytical approximation of the two-dimensional percolation threshold for fields of overlapping ellipses", Physical Review E, **66**, pp. 066130-1 – 066130-8.

102. **Kojima, Y., Usiki, A., Kawasumi, M., Okada, A., Fukushima, Y., Karauchi, T., and Kamigaito, O.**, (1993), "Mechanical Properties of Nylon-6 Clay Hybrids", Journal of Material Research, **6**, pp. 1185-1189.

103. **Kato, M., Y., Usiki, A., and Okada, A.,** (1997), "Synthesis of Polypropylene Oligomer-Clay Intercalation Compounds", Journal of Applied Polymer Science, **66**, pp. 1781-1785.

104. **Kawasumi, M., Hasegawa, N., Kato, M. Y., Usiki, A., Okada, A., Karauchi, T., and Kamigaito, O**., (1997), "Preparation and Mechanical Properties of Polypropylene-Clay Hybrids", Macrocmolecules, **30**, pp. 6333-6338.

105. **Lau, K**., **Ho, M., Lam, C., H.L. Ng, D., Hui, D.,** (2006), "Mechanical Properties of Epoxy-based Composites using Nanoclays", Composite Structures, **75**, pp. 415-421.

106. **Chow W. S., and Bakar, A. A.,** (2005), "Effect Of Maleic Anhydride-Grafted Ethylene–Propylene Rubber On The Mechanical, Rheological And Morphological Properties Of Organoclay Reinforced Polyamide6/Polypropylene Nanocomposites", European Polymer Journal, **41**, pp. 687-696.

107. **Gilman, J. W., and Alexander B. A**., (2003), "Characterisation of Polymer-Layered Silicate (Clay) Nanocomposites by Transmission Electron Microscopy and X-Ray Diffraction: A Comparative Study", Journal of Applied Polymer Science, **43**, pp. 1329-1338.

108. **H. Cai, F. Yan E., Xue Q., and Liu W.**, (2003), "Investigation of tribological properties of Al2O3-polyimide nanocomposites", Polymer Testing, **22**, pp. 875-882.

109. **Shi, G., Zhang M.Q., Rong M.Z., Wetzel B., and Friedrich K.**, (2004), "Sliding wear behavior of epoxy containing nano-Al2O3 particles with different pretreatments", Wear, **256**, pp. 1072–1081.

110. **Wang, Q. H.**, **Xu J., Shen W., and Xue Q.,** (1997), "The effect of nanometer SiC filler on the tribological behavior of PEEK", Wear, **209,** pp. 316-321.

111. **Shwartz C. J., and Bahadur S.**, (2000), "Studies on the tribological behavior and transfer film–counterface bond strength for polyphenylene sulfide filled with nanoscale alumina particles. Wear, **237**, pp. 261-273.

112. **Khedkar J., Negulescu L., and Meletis E.I.**, (2002), "Sliding wear behavior of PTFE composites", Wear, **252**, pp. 361–369.

113. **Ray, S. S., and Okamoto, M.**, (2003), "Polymer/layered silicate nanocomposites: a review from preparation to processing", Polymer Science Journal, **28**, pp. 1539-1641.

114. **Fornes, T. D., Yoon, P. J., and Paul, D. R.**, (2003), "Formation and properties of Nylon 6 nanocomposites", Polímeros: Ciência e Tecnologia, **14**, pp. 212-217.

.

LIST OF PAPERS PUBLISHED ON THE BASIS OF THIS THESIS

I REFEREED JOURNALS

1. **V. K. Moodley, K. Kanny,** (2007), "Characterisation of Polypropylene Nanocomposite Structures", **Journal of Engineering Materials and Technology**, **40**, pp. 1 – 8.

2. **K. Kanny**, **P. Jawahar**, **V. K. Moodley**, "Mechanical and Tribological Behaviour of Clay-Polypropylene Nanocomposites", communicated to **Journal of Material Science.**

II PRESENTATIONS IN CONFERENCES

1. **V. K. Moodley, K. Kanny, "**Nano Modified Thermoplastics" ***Composites Africa 2004,*** Polymeric Composites Institute of South Africa (PCISA), Caesars, Gauteng, August 2004.

2. **V. K. Moodley, K. Kanny, "**Synthesis, Mechanical Properties And Fracture Surface Morphology Of Nano-Infused Polypropylene" ***ICCM 15,*** Paper Ref: **P020**, Polymeric Composites Institute of South Africa (PCISA), Caesars, Gauteng, August 2005.

3. **V.K. Moodley**, **S. Pillay** and **K. Kanny, "**Mechanical behavior of polypropylene montmorillonite nanocomposites", Research Day 2005, Durban Institute of Technology, Old Mutual Lecture Theatre, Ritson Road Campus.

4. **K. Kanny, S. Pillay, V.K. Moodley, A. Ramsaroop, Y. Li, P. Dilsani, "**On A Hybrid Composite Pedestrian Bridge", Research Day 2005, Durban Institute of Technology, Sport Centre.

5. **V. K. Moodley, K. Kanny, "**Nano-infused Polypropylene-Composite Structures", ***First Annual Ledger Conference Agenda 2005,*** The Council of Scientific and Industrial Research (CSIR) and Denel Aerospace Systems (DAS), 2005.